UNIVERSITY OF CALIFORNIA
IRVINE

In-Vitro Fatigue Behavior of Different Materials Used as Frontalis Suspension Slings for Treatment of Blepharoptosis

DISSERTATION

Submitted in partial satisfaction of the requirements
for the degree of

DOCTOR OF PHILOSOPHY

in Biomedical Engineering

by

Omid Rohani

Dissertation Committee:
Professor James C. Earthman, Chair
Professor Jeremiah Tao
Professor James Brody

2017

DEDICATION

To

My wife, Mona, for your unending support and for the infinite levels of sacrifice you've displayed. Without you none of this would be possible.

To my dear family,

for their endless encouragement and support.

"We should be taught not to wait for inspiration to start a thing. Action always generates inspiration. Inspiration seldom generates action." - Frank Tibolt

TABLE OF CONTENTS

LIST OF FIGURES

LIST OF TABLES

ACKNOWLEDGMENTS

I would like to express my special appreciation and thanks to my advisor Professor James Earthman, who has been a tremendous mentor for me. I would like to thank him for encouraging my research and for allowing me to grow. I also owe a great deal to Professor Jeremiah Tao for being my mentor and giving insights during this research. I would also thank Professor James Brody for all his support and guidance during my graduate studies in Biomedical Engineering.

I want to remember and thank Prof. Roger Steinert. He was an internationally renowned and respected ophthalmologist. His support especially during the conception of this research was truly helpful. We unfortunately missed him this summer.

I want to appreciate the contribution from Dr. Matin Khoshnevis, Dr. Jeffrey M. Joseph, and Dr. Marc Yonkers from the Gavin Herbert Eye Institute towards this research. I would also like to thank the UCI Biomedical Engineering Department faculty and staff. I want to thank Steve Weinstock, Ted Hes, and Tucker Parris in the Engineering machine shop at UCI. I would also like to thank the undergraduate students from Earthman's lab who helped with this project: Cristian Hernandez, Xavier Chuck, and especially Ali Aboughaida.

Lastly, I appreciate and acknowledge my everlasting support system – my close family. I am grateful of the continuous support I've received from my wife and dearest friend, Mona; my family; and Mona's family.

CURRICULUM VITAE

Omid Rohani

109 Engineering Tower **(949) 981-0303**
Irvine, CA 92617 **orohani@uci.edu**

RESEARCH INTERESTS

Fatigue analyses of ocular implants
Engineering-guided oculoplastic surgery
Biomaterials for oculoplastic surgery
Biomechanical studies of medical devices
Cataract Surgery Instrumentation
Engineering Pedagogy

EDUCATION

Ph.D. Biomedical Engineering September 2017
University of California, Irvine
PhD Thesis: In-Vitro Fatigue Behavior of Different Materials Used as Frontalis Suspension Slings for Treatment of Blepharoptosis
Advisor: James C. Earthman, Ph.D.
GPA: 4.0/4.0

M.S. Biomedical Engineering January 2012
University of California, Irvine
MS Thesis: Modeling and Experimental Verification of Piezoelectric Transducers for *in vitro* cell biomechanics
Advisor: William Tang, Ph.D.
GPA: 4.0/4.0

M.S. Mechanical and Aerospace Engineering March 2011
University of California, Irvine
MS Thesis: Design and Implementation of a Path Tracking System on a Rotary Platform
Advisor: Marc Madou, Ph.D.
GPA: 3.6/4.0

B.S. Mechanical Engineering June 2006
University of Tehran, Iran
BS Thesis: Analysis of Moving Loads on the Surface of a Cylindrical Bore
Advisor: Nikkhah-Bahrami, Ph.D.
GPA: 18.05/20

PUBLICATIONS and PATENTS

Omid Rohani, Matin Khoshnevis, Jeremiah P. Tao, James C. Earthman, "An Experimental Study of the Effects of Cyclic Loading on Fascia Lata and Silicone Slings in Frontalis Suspension", American Academy of Ophthalmology, November 2016

Omid Rohani, Aghil Yousefi-Koma, Ayyoub Rezaeeian, Alireza Doosthoseini, "Force Control of a Shape Memory Alloy Wire Using Fuzzy Controller", Proceeding of SPIE Vol. 6926, 692611, 2008 Modeling, Signal Processing, and Control for Smart Structures

Alireza Doosthoseini, Aghil Yousefi-Koma, Behrouz Shasti, **Omid Rohani,** "Fuzzy Control of a Flexible Structure Using Piezoelements", Proceeding of SPIE Vol. 6926, 692612, 2008 Modeling, Signal Processing, and Control for Smart Structures

M. Nikkhah-Bahrami, A. Hajati**, O. Rohani**, "Analysis of Moving Loads on the Surface of a Cylindrical Bore using Neural Network", Intl. Symposium on Neural Networks & Soft Computing in Structural Engineering, Krakow, Poland, 2005

O. Rohani, H. Rohani, "Intelligent Glasses Finder", Iranian Patent No. 32854, 2005

TEACHING EXPERIENCE

Instructor and Teaching Assistant, University of California, Irvine 2008 – 2017

- *Teaching Assistant, Biomechanics III (BME 110C)* (Spring 2017)
  Developed course materials for discussion and review sessions, delivered discussion sessions, held review sessions, developed grading protocol, graded homework, and examinations, kept student/course records, managed the course website, held office hours.

- *Instructor, Introduction to Engineering (ENG 7B)* (Winter 2017)
  Taught fundamentals of engineering through the design, manufacture and testing of Wearable Fitness Tracker; Guided small teams of freshman and sophomore engineers to develop, build, code and test their own version of fitness tracker; The project involved Arduino, circuit design, electrical fabrication, Solidworks design, and 3D printing.

  Developed course materials for lecture and lab sessions, delivered lectures, held lab sessions, developed grading protocol, graded homework, project reports and examinations, kept student/course records, managed the course website, held office hours

- *Teaching Assistant, Introduction to Engineering (ENG 7A)* (Fall 2016)
  Guided small teams of freshman engineers to design, build, and test their own quadcopter; The project involved Arduino, circuit design, electrical fabrication, Solidworks design, and mechanical fabrication.

  Held lab sessions and office hours, assessed students' presentations, kept student/course records.

- *Instructor, Introduction to Engineering* (Summer 2016)
  Taught fundamentals of engineering through the design, manufacture and testing of Wearable Fitness Tracker; Guided small teams of sophomore and junior engineers to develop, build, code and test their own version of fitness tracker; The project involved Arduino, circuit design, electrical fabrication, Solidworks design, 3D printing, algorithm and mobile app development. This course was offered as a substitute for an internship in the industry to a selected group of students from KAUST University.

  Developed course materials for lecture and lab sessions, delivered lectures, held lab sessions, kept student/course records, held office hours

- *Teaching Assistant, Biomechanics III (BME 110C)* (Spring 2016)
  Developed course materials for discussion and review sessions, delivered discussion sessions, held review sessions, developed grading protocol, graded homework, and examinations, kept student/course records, managed the course website, held office hours.

- *Teaching Assistant, Biomechanics I (BME 110A)* (Fall 2015)

Developed course materials for discussion and review sessions, delivered discussion sessions, developed grading protocol, graded homework, and examinations, kept student/course records, held office hours.

- *Teaching Assistant*, *Biomedical Engineering Laboratory (*Spectrometry and Pulse Oximetry Lab*) (BME 170)* (Spring 2015)
  Lectured in and conducted the lab sessions, supervised students in the laboratories, developed grading protocol, graded lab reports and examinations, kept student/course records, held office hours.

- *Teaching Assistant*, *Biomechanics I (BME 110C)* (Fall 2014)
  Developed course materials for discussion and review sessions, delivered discussion sessions, delivered a lecture instead of the course instructor, developed grading protocol, graded homework, and examinations, kept student/course records, held office hours.

- *Teaching Assistant*, *Biomedical Engineering Laboratory (*Human NeuroEngineering Lab--Auditory System) *(BME 170)* (Spring 2014)
  Lectured in and conducted the lab sessions, supervised students in the laboratories, developed grading protocol, graded lab reports and examinations, kept student/course records, held office hours.

- *Teaching Assistant*, *Mechanics of Structures (ENG/MAE 150)* (Summer 2013)
  Developed course materials for discussion and review sessions, delivered discussion sessions, developed grading protocol, graded homework and examinations, created and maintained the course website, kept student/course records, held office hours.

- *Teaching Assistant*, *Biomechanics III (BME 110C)* (Spring 2013)
  Developed course materials for discussion and review sessions, delivered discussion sessions, developed grading protocol, graded homework, reports and examinations, kept student/course records, managed the course website, held office hours.

- *Teaching Assistant*, *Biomechanics II (BME 110B)* (Winter 2013)
  Developed course materials for discussion and review sessions, delivered discussion sessions, developed grading protocol, graded homework, reports and examinations, kept student/course records, held office hours.

- *Teaching Assistant*, *Biomechanics I (BME 110A)* (Fall 2012)
  Developed course materials for discussion and review sessions, delivered discussion sessions, delivered a lecture instead of the course instructor, developed grading protocol, graded homework, reports and examinations, kept student/course records, held office hours.

- *Teaching Assistant*, *Design of Biomedical Electronics (BME 140)* (Winter 2010)
  Developed course materials for discussion and review sessions, delivered discussion sessions, lectured in and conducted the lab sessions, developed grading protocol, graded homework, lab reports and examinations, kept student/course records, held office hours.

- *Teaching Assistant*, *Mechanics of Structures (ENG/MAE 150)* (Fall 2008)
  Developed course materials for discussion and review sessions, delivered discussion sessions, developed grading protocol, graded homework and examinations, created and maintained the course website, kept student/course records, held office hours.

- *Teaching Assistant, Heat Transfer (MAE 120)* (Summer 2008**)**
  Developed course materials for discussion and review sessions, delivered discussion sessions, developed grading protocol, graded homework and examinations, made exam questions, kept student/course records, held office hours.

Teaching Assistant, University of Tehran 2004 - 2006
Developed course materials for discussion and review sessions, delivered discussion sessions, made exam questions, developed grading protocol, graded homework, kept student/course records.

- *Dynamics* (Fall semester 2005, Fall semester 2004)
- *Mechanical Vibrations* (Spring semester 2005)
- *Automatic Control* (Fall semester 2005)

Director and lecturer, NODET*, Isfahan, Iran — Summer 2002
Organized and lectured at the "NODET* 4th Workshop on Physics for high school students
National Organization for Development of Exceptional Talents

Instructor — Fall 1999 – Fall 2001

Taught "Physics for Olympiad" to high school students at NODET* high school

INVITED PRESENTATIONS

"Fatigue of Implants Used for Droopy Eyelids Corrective Surgeries", Alcon Surgical Instruments R&D Invited Presentation, Alcon Laboratories, Lake Forest — July 2017

Guest Lecture, Biomaterials (BME 111) course, University of California, Irvine — April 2016

Guest Lecture, Biomechanics I (BME 110A) course, University of California, Irvine — December 2014

"Microplatforms for Cardiomyocyte Biomechanics", Edwards Lifesciences Center for Advanced Cardiovascular Technologies, Irvine — January 2013

Guest Lecture, Biomechanics I (BME 110A) course, University of California, Irvine — October 2012

"Force Control of a Shape Memory Alloys Wire", University of California, Irvine — October 2007

RESEARCH EXPERIENCE

Research Assistant — Summer 2013 - Present
Gavin Herbert Eye Institute,
University of California, Irvine
& Mechanical Behavior of Biomaterials Lab, Biomedical Engineering Dept., University of California, Irvine

- Developed two novel experimental setups for investigating the occurrence of plastic elongation in the eyelid slings
- Developed a laser scanning system for plastic strain monitoring in tissues and suture-like materials
- Evaluated eyelid suspension grafts under cyclic loading conditions (fatigue analysis)
- Developing novel eyelid slings
- Mentored three undergraduate students on their projects related to this research trust

Research Assistant for Prof. William Tang — Summer 2011 - Summer 2013
Microbiomechanics Lab, Biomedical Engineering Dept.,
University of California, Irvine

- Microfabricated an Environment for Simulating the Rheology of Blood Capillaries
- Microfabricated a Piezoelectric Microplatform for Cellular Diagnostics
- Simulated Cells responses to Piezoelectric Beam Deformations using Finite Element Analysis
- Evaluated Piezoelectric Microplatforms Experimentally
- Mentored tow undergraduate students on their projects related to this research trust

Research Assistant for Prof. Abraham Lee — Winter 2011 - Spring 2011
BioMINT Lab, Biomedical Engineering Dept.,

University of California, Irvine
- Designed and Tested Air-Liquid Cavity Acoustic Transducers for Lab-on-a-Chip Applications

Research Assistant for Prof. Marc Madou Spring 2008 - Fall 2010
BioMEMS Lab, Mechanical and Aerospace Engineering Dept.,
University of California, Irvine
- Designed, manufactured, and Implemented a Path Tracking System on a Rotary Platform
- Developed a Controlling Application for the Implemented System using LabVIEW Software

Research Assistant for Prof. Yousefi-Koma Fall 2005 - Summer 2007
Advanced Dynamic and Control Systems Lab, School of Mechanical Engineering,
University of Tehran
- Designed an Experimental Setup for Controlling Smart structures such as Shape Memory Materials
- Added a Fuzzy Logic Controller to Provide Custom Control of the Setup

Research Assistant for Prof. Nikkhah-Bahrami Fall 2004 - Fall 2006
School of Mechanical Engineering, University of Tehran
- Analytically Derived Equations Governing the Dynamics of Moving Loads on the Surface of Cylindrical Bores
- Implemented the Equations Numerically using MATLAB and Neural Networks

UT Rescue and Sumo Robot team member Winter 2005 - Summer 2005
Control and Robotics Lab, School of Mechanical Engineering,
University of Tehran
- Designed and Manufactured Sumo and Rescue Robots

Researcher Fall 2002 – Fall 2006
Isfahan Fertility and Infertility Center, Prof. Ahmadi, M.D.
- Studied Biological Effects and Potential Hazards of Radiation, with Special Attention to Possible Effects of Microwaves Used in Cellular Phone System on Infertility

TECHNICAL EXPERIENCE

Alcon, a Novartis Company, *Lake Forest, CA* September 2016-December 2016
Internship
Characterization of occlusion break surge in cataract surgical instruments

Zarif Polymer Co., *Isfahan, Iran* Summer 2005
Internship
Configuration enhancement of the machines in the Product Line

HONORS and AWARDS

People's Choice Award, AGS Symposium, April 2016
Celebrating graduate student research at UCI

Best Poster-3rd place Award and People's Choice Poster Award, April 2016
Graduate Poster Contest, ASM International Los Angeles Chapter

Pedagogical Fellowship, University of California, Irvine 2013-2014

Research/teaching assistantship, University of California, Irvine Department of Biomedical Engineering Fall 2011-present

Fellowship and research/teaching assistantship, University of California, Irvine; Department of Mechanical and Aerospace Engineering Fall 2007-Spring 2011

Awarded "FOE (Faculty Of Engineering)" prize for the highest GPA in the School of Engineering, University of Tehran 2003, 2004, 2005

1st Ranked among University of Tehran Mechanical Engineering graduates of 2006 2006

Awarded "*the Europe Tour for Top Students*" by *University of Tehran* 2006

Scholarship, University of Tehran 2001-2006

Scholarship, Isfahan University of Medical Sciences 2001-2006

Awarded "*Kayson**" prize for the highest GPA in the School of Engineering, University of Tehran 2004
**Kayson is the pioneer EPC contractor in the gas & oil section in Iran, providing world-class design, management, procurement and construction services.*

Silver Medal, 14thNational Physics Olympiad 2001

COMPUTER SKILLS

Programming: C++, Pascal, QuickBASIC, R, Python
Engineering: Solidworks, Mechanical Desktop, AutoCAD, L-Edit, ADAMS, ANSYS, ABAQUS, FLUENT, Comsol, CFD RC, MATLAB, Simulink, LabView, Mathematica
OS: Dos, Windows, OS X, Linux
Other: Microsoft Office, Adobe Illustrator, Adobe Photoshop

PROFESSIONAL EDITING EXPERIENCE

Editing Assistant**, *"Fundamentals of Microfabrication and Nanotechnology"*** book by Marc J. Madou 2008

Editing Assistant**, *"Vectorial Dynamics"*** book by Mansour Nikkhah-Bahrami 2004-2006

PROFESSIONAL DEVELOPMENT CERTIFICATES

Excellence in Engineering Communications, Graduate Division, University of California, Irvine May 2016

SciPhD Certificate Program- Core Professional Skills That Make You competitive for a Professional Career Sep. 2015

Mentoring Excellence Program, Graduate Division, University of California, Irvine May 2015

Advanced Pedagogy and Academic Job Preparation, University of California, Irvine 2012-2014

PROFESSIONAL MEMBERSHIPS

Institute of Electrical and Electronics Engineers (IEEE), Engineering in Medicine & Biology Society

Biomedical Engineering Society

American Society of Mechanical Engineers

ASM International

Minerals, Metals, and Materials Society

SERVICES

Teaching Assistant Professional Development Program — Sept 2013 and Sept 2015
University of California, Irvine
Prepared and conducted a two-day long specific to the discipline and practice-oriented training series of workshop for all UCI engineering teaching assistants

Lab safety Representative, Mechanical Behavior of Biomaterials Lab and Fatigue Lab — Winter 2015-present
University of California, Irvine
Coordinated with University officials on all lab member safety issues, managed records of lab safety protocols

Mentoring High School Students in Math and Science — 2013
Elite Educational Institute, Mission Viejo, CA

ABSTRACT OF THE DISSERTATION

In-Vitro Fatigue Behavior of Different Materials Used as Frontalis Suspension Slings for Treatment of Blepharoptosis

By

Omid Rohani

Doctor of Philosophy in Biomedical Engineering

University of California, Irvine, 2017

Professor James C. Earthman, Chair

Frontalis suspension is a commonly used surgery that is indicated in patients with droopy eyelids (blepharoptosis) and poor levator muscle function. The surgery is based on connecting the tarsal plate of the droopy eyelid to the frontalis muscle with various slings made either from fascia lata tissue or synthetic materials. However, one of the main complications of this surgery is the high rate of blepharoptosis recurrence, which has been reported for some slings as high as 100%.

We initiated a collaborative multidisciplinary research to explore the effect of choice of sling material on this common problem. Two different experimental setups for testing the behavior of various sling materials in-vitro have been developed. Using our first experimental setup, we explored possible gradual permanent elongation of sling materials due to cyclic loading caused by eye blinking. In addition, a more sophisticated second experimental setup was developed to investigate fatigue behavior of different implants under physiologically relevant conditions.

We could show that physical changes such as permanent elongation, and holding load drop in the slings could happen under fatigue conditions caused by eye blinking. These changes can contribute to the failure of the frontalis suspension slings and recurrence of blepharoptosis. Our experiments show that different sling materials exhibit significantly different responses. The results of the present study indicate that characterizing the in vitro fatigue behavior of different sling materials can lead to a better understanding of what causes high recurrence rates in frontalis suspension. The characterization methods developed can also be used to improve material selection as well as assist in the development of new materials for this procedure.

Chapter 1

Introduction and Background

Ptosis

“Ptosis” (also known as “droopy eyelids” or in its exact term “Blepharoptosis”) is referred to drooping of the upper eyelid. This problem can be found in all age groups and has various etiologies. Ptosis is one of the most prevalent eyelid disorders encountered in ophthalmology. It generally is classified to congenital ptosis (present at birth or within the first year of life) or acquired ptosis (present after the age of one year). Ptosis can be unilateral (present only in one eye) or bilateral (present in both eyes) [1], [2]. Figure 1 shows congenital and acquired ptosis in two patients.

Congenital ptosis

The most common origin of congenital ptosis is myogenic due to the improper development of the levator muscle. Congenital ptosis may result is amblyopia (or lazy eye) which can cause severe consequences such as brain development problems in children. Amblyopia which is more common in kids with unilateral congenital ptosis [3], can be developed in around 20–70% of patients with simple congenital ptosis [4], [5]. Ptosis can also lead to visual loss in adults due to partial or complete obstruction of the pupil and hence the visual field [6].

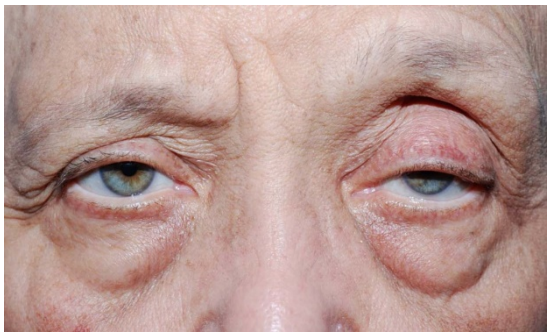

(A) (B)

Figure 1: Congenital and acquired ptosis cases: (A) a 3-year old patient with unilateral congenital ptosis in upper left eyelid – picture source: [5] (B) A patient with bilateral acquired ptosis. Here, ptosis in the left eye is more significant - picture source: Eyewiki [7]

Acquired ptosis

Acquired ptosis can have myogenic, aponeurotic, neurogenic, mechanical or traumatic reasons. In myogenic ptosis, elevation of the upper eyelid to the appropriate position is prevented by malfunction or dysfunction of the levator muscle. The most common disease causing myogenic ptosis are myotonic dystrophy, congenital myopathies, myasthenia gravis, and oculopharyngeal muscular dystrophy[8].

Aponeurotic ptosis can be seen in both children and adults. In children, birth trauma following forceps delivery or failure of the aponeurosis to insert on the anterior surface of the tarsus can cause congenital aponeurotic ptosis. On the other hand, abnormality in the levator aponeurosis, such as its stretching or disinsertion is the most common cause of acquired ptosis in adults. Stretch of levator muscle and its aponeurosis in adults can be occurred due to the effects of loss of tone in the muscle or effects of the gravity [9].

Neurogenic ptosis can be mainly caused from damages and dysfunction that directly happens to the cranial nerve III (oculomotor nerve), which innervates the levator muscle or indirectly is caused through neurological diseases such as multiple sclerosis (MS), diabetes, or presence of tumors [2], [8].

Mechanical ptosis is caused by excess weight of the upper eyelid. In this case, the eyelid is too heavy for the muscles to be lifted. The extra weight could be caused by excessive skin, mass or tumors in the eyelid [10].

In traumatic ptosis, the levator may be transected or disinserted due to an eyelid injury or fracture of the orbital roof with foreign bodies. Transection of the levator muscle and its tendon can also lead to scar formation and secondary mechanical ptosis [11].

In contrary to the aforementioned cases, the appearance of ptosis in the absence of levator abnormality is referred to as *pseudoptosis* [2], [12].

Epidemiology and statistics

With respect to the statistics and epidemiology of ptosis, equal frequency among different races and equal frequency between the sexes have been reported. Also, as discussed earlier, ptosis may present within a broad range of a human's lifetime [13]. The prevalence of ptosis among youth who are 12-17 years old has been reported as 1.9 cases per 1,000 youths in the non-institutionalized population of the United States [14]. On the other hand, ptosis has been increasingly recognized in the elderly population, particularly after cataract extraction or lens replacement [15]. Aging, diabetes, myasthenia gravis, brain tumor, or cancer, which can affect nerve or muscle response are some of the risk factors for developing ptosis [13].

Symptoms and signs

In order to diagnose blepharoptosis, clinical examination is sufficient in most of the patients. Visual field is also usually tested to check for the impact of ptosis on patient's vision. However, in few patients imaging studies and laboratory tests are needed to figure out cause of blepharoptosis [12]. The drooping of the eyelid in ptosis maybe hardly evident, or the eyelid can descend over all the pupil. If the droopy eyelid covers parts or all the pupil, the patient suffers from partial or complete visual field loss. The patient may also complain of blurred vision or increase tearing [13]. Furthermore, ptosis disturbs the quality of life of patients by interfering with their daily life activities such as reading, climbing the stairs, and driving. Most ptosis patients complain about having a sleepy or tired appearance [2]. It has been shown by Bullock et al. that members of society seem people with ptosis negatively and associate to them less positive characteristics such as intelligence, hard work, and trustworthiness in comparison with healthy people [16]. Other related complaint include prefrontal headaches due to chronic use of the frontalis muscle in an attempt to lift the eyelids [17].

Treatment of ptosis

According to severity, ptosis may be minimal or mild (1–2 mm), moderate (3–4 mm), or severe (>4 mm) [13], [18]. Ptosis treatment is governed by age, etiology, whether it is unilateral or bilateral, its severity, presence of additional ophthalmologic or neurologic abnormalities, and the levator function.

Generally, treatment of ptosis includes a watch-and-wait policy, prosthesis, medication, botulinum toxin (Botox) injections, or surgery. Classically, patients with good levator muscle function undergo levator aponeurosis advancement procedure, which tightens or reattaches the aponeurosis

back to the tarsal plate. Patients with weak levator muscles undergo a frontalis sling procedure in which the upper eyelid tarsus is connected to the frontalis muscle, allowing them to open the eyelid using the frontalis muscle located in the brow area [13], [19].

Although not commonly used and suggested, ptosis eye crutches can sometimes also be used to address ptosis. They are tools and bars installed to existing glasses along the inside of an eyewire frame to support the ptotic eyelid and enable it to stay open [20].

Risks of ptosis surgery occasionally include infection, bleeding, over- or undercorrection, and reduced vision. There may be short-term difficulties in completely closing the eye straightaway after surgery. However, postoperative healing may lift the lid to an undesired variable extent. Sometimes, even when enhancement of the eyelid height is accomplished, the eyelids may not look like seamlessly symmetrical. There are cases that more than one surgery is needed. [13]. The reoperation rate in most cases of general acquired ptosis differs from 5% to 35%. [17]

Upper Eyelid anatomy

In this section, we just review the anatomical features and terminologies that are relevant to the scope of this dissertation. The upper eyelid is mainly elevated by the palpebrae superioris muscle. However, in more detail, the elevators of upper eyelid are the levator palpebrae superioris muscle and the Muller's muscle. The levator palpebrae superioris (referred to levator muscle in this dissertation) is the predominant upper eyelid elevator and is innervated by the cranial nerve III (oculomotor nerve). The Muller's muscle is a smooth muscle that is innervated by the sympathetic nervous system and is responsible for the over-elevation of the eyelid when a person becomes excited or fearful (see Figure 2 for a cross section of the upper eyelid and the muscles attached to it).

The closure of the eyelid is enabled by the eyelid protractor which is different from the elevators of upper eyelid. Orbicularis oculi muscle is the eyelid protractor and is innervated by the cranial nerve IV (facial nerve). Interestingly, orbicularis muscle is the fastest muscle in the body [21]. In sum, different muscles which are innervated from different nerves are responsible for opening and closing of the eyes [2]. The key muscles that are responsible for opening and closing the eyelid and blinking are shown in Figure 3.

Also, frontalis muscle needs to be mentioned here. The frontalis muscle lifts the brows and therefore can be a minor contributor to eyelid retraction. It is innervated by cranial nerve VII (facial nerve). Patients with ptosis will often lift their brows to slightly elevate their eyelids, which consequently may result in a brow ache and headache from overuse [22].

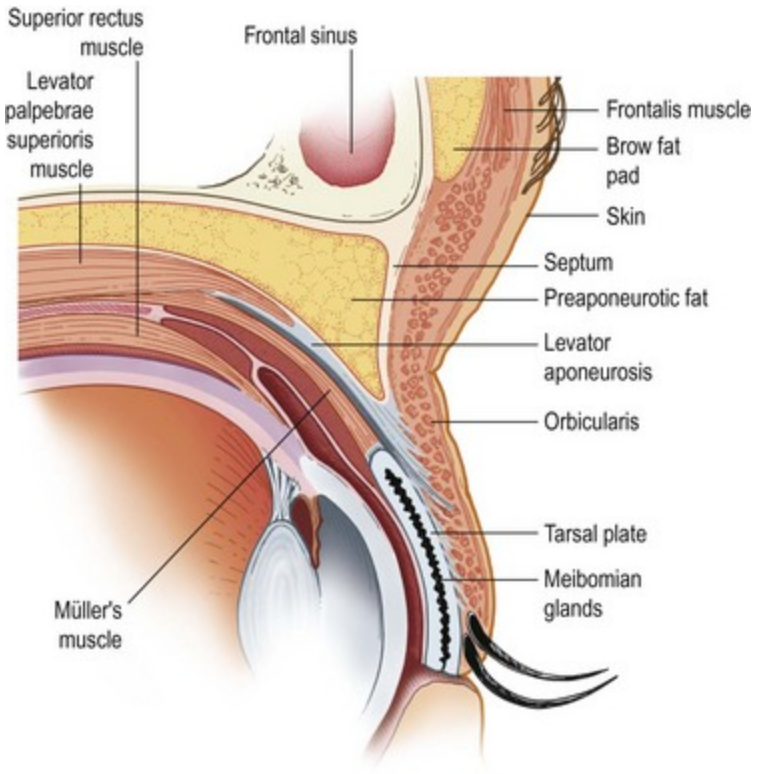

Figure 2: Cross-section of the upper eyelid - picture source: https://clinicalgate.com/eyelid-anatomy-and-function/ [23]

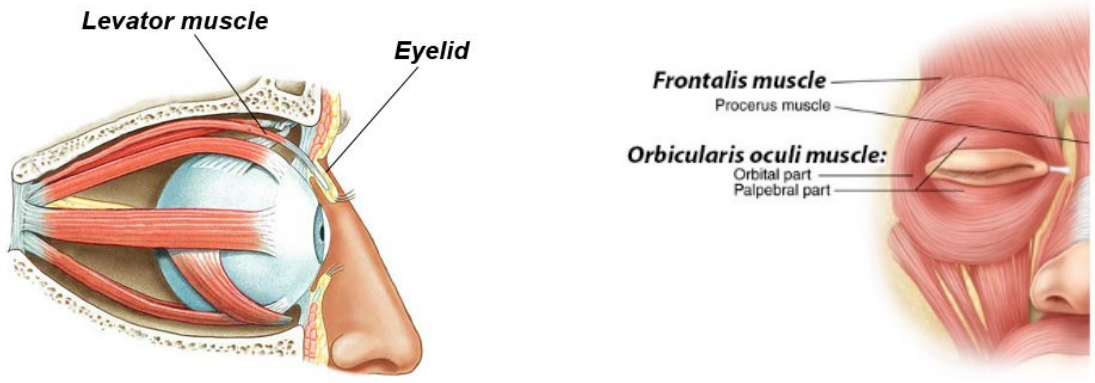

(A) (B)

Figure 3: The key muscles for opening and closing the eye: (A) levator muscle for opening the eye, (B) orbicularis oculi for closing the eye. Frontalis muscle is also shown in this picture - picture source: Wolters Kluwer Health Lippincott Williams & Wilkins

Levator function

The appropriate method of ptosis surgery is determined by levator function, degree of ptosis and preference. [24]–[26]. In order to measure the levator function, the physician firmly places a finger on the patient's brow to cancel the effects of the frontalis muscle. Then the patient is asked to gaze downward. A ruler is placed at the upper lid margin. Next the patient is asked to gaze upward and the new position of the upper lid is measured. The distance between the two measurements is considered as the levator function (LF) (see Figure 4 below). Normal levator function is 13-17 mm. [22]

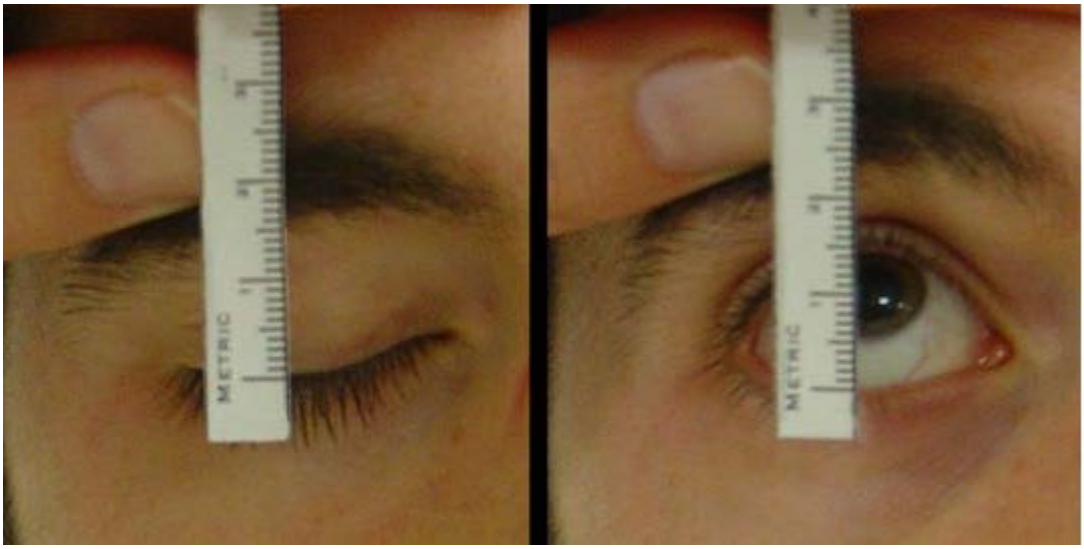

Figure 4: Measurement of levator function (LF) with the patient in downgaze (left) and upgaze (right) – picture courtesy of [27]

Numerous studies have examined these factors. However, levator function is regarded as the most discernible predictive factor [28], [29] and a key defining factor in picking the appropriate surgical procedure for ptosis correction irrespective of the etiology and degree of ptosis.[30].

Frontalis suspension procedure is traditionally indicated for severe ptosis cases with poor LF (0–4 mm) while levator resection techniques are usually reserved for ptosis with fair (5–7 mm) to good LF (>8 mm). [26], [29].

Marginal Reflex Distance

The marginal reflex distance-1 (MRD-1) is the distance between the center of the pupillary light reflex and the upper eyelid margin with the eye in primary gaze while the marginal reflex distance-2 (MRD-2) is the distance between the center of the pupillary light reflex and the lower eyelid margin with the eye in primary gaze. (see Figure 5)

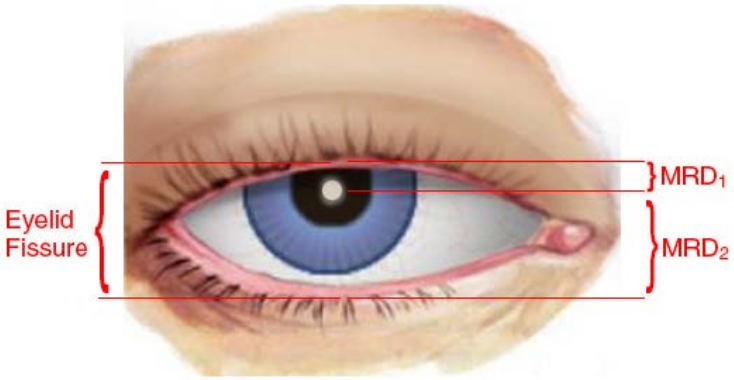

Figure 5: Measurement of MRD1 and MRD2

Margin-reflex distance (MRD) has also been utilized as an alternative to levator function (LF) in choosing the suitable surgical procedure for congenital ptosis. The MRD at the cutoff point of 0.5 mm may be used as an alternative to LF to determine the type of suggested surgical intervention in patients with congenital ptosis whose LF cannot be unfailingly found in clinical evaluations. [31]. Moreover, Cetinkaya and Brannan evaluated the findings of the previous studies on ptosis surgical correction and suggested an algorithm for appropriate surgical selection with utilization of both LF and MRD1 parameters. [32]

Frontalis Suspension

When there is a poor (<4mm) or absent function of levator palpebrae superioris muscle in lifting the upper eyelid or when there is severe ptosis (>4 mm of droop relative to the “normal”), the resulting ptosis is addressed by performing a brow-suspension or frontalis suspension surgery. Also, this procedure is indicated in the case of myogenic ptosis, neuromuscular diseases, and where linkage between the muscle and the eyelid is abnormal (such as Marcus Gunn jaw-winking phenomenon).

During this procedure, the droopy upper eyelid is subcutaneously connected by an implanted cord-like sling to the frontalis muscle, which is located on the forehead and above the eyebrows. Performing this procedure allows the patient to perform the eyelid elevation with the use of the frontalis muscle. Figure 6 schematically shows how the upper eyelid is connected to the frontalis muscle in this procedure.

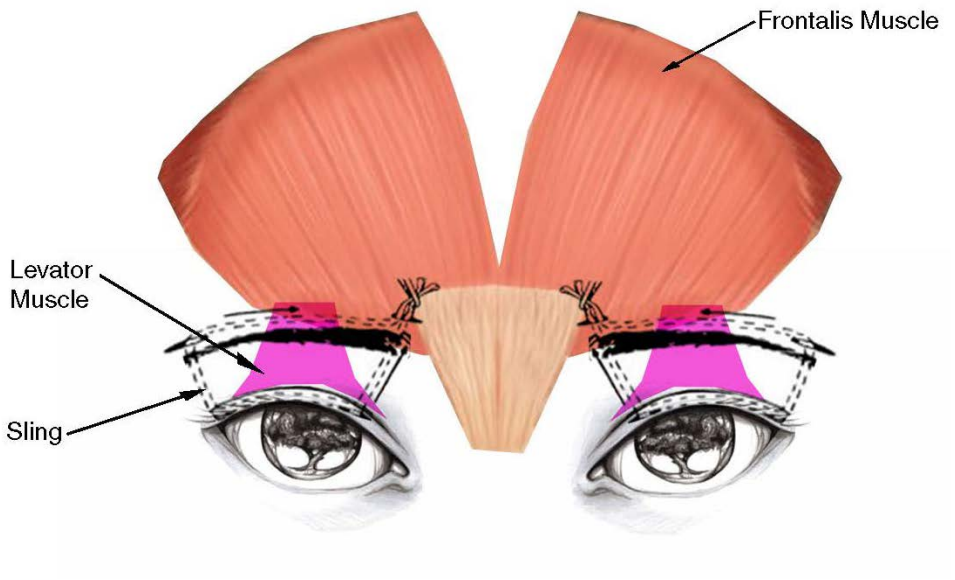

Figure 6: Frontalis muscle suspension procedure: in frontalis suspension surgery, the upper eyelid is connected by a sling to the frontalis muscle, allowing opening of the eyes with the help of frontalis muscle in lieu of levator muscle. The trapezoid sling design has been utilized here.

Frontalis suspension sling materials

The implanted sling for frontalis suspension blepharoptosis repair could be made out of a wide variety of materials. Common materials include fascia lata (fresh or processed/banked), nylon suture and silicone filament [33]. However, other materials such as collagen, chromic gut, silk, steel, polypropylene, polyester, and polytetrafluoroethylene (PTFE) have been also reported to be used for this procedure [34-37].

Frontalis suspension sling designs

A number of patterns and designs have been described for the passage of the suspension sling material, such as a single triangle [34], double or multiple triangle (Crawford triangles) [24], [35], rhomboid [36] [37] , double trapezoid [38], and pentagon (Fox pentagon) [39].The most commonly

used configurations are Crawford triangles and Fox pentagon. [40]. Figure 7 shows three methods for sling design and geometry.

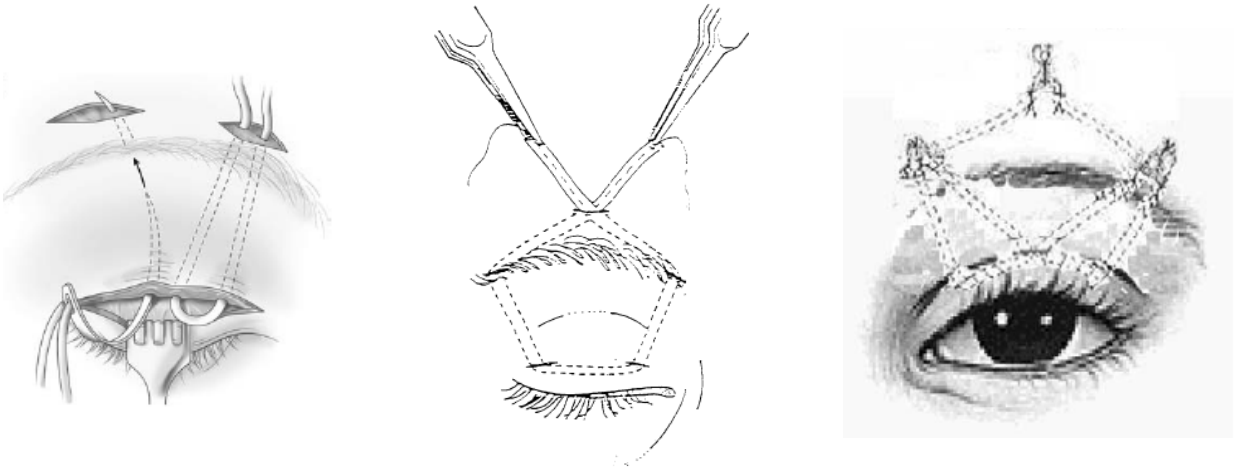

A B C

Figure 7: Three different surgical designs for frontalis suspension: (A) Crawford Triangles – picture source: [17], (B) Fox Pentagon – picture source: [41], and (C) double pentagon – picture source: [5]

The following figure shows how performing a frontalis suspension procedure on a patient suffering congenital ptosis has alleviated the droopy eyelid issue.

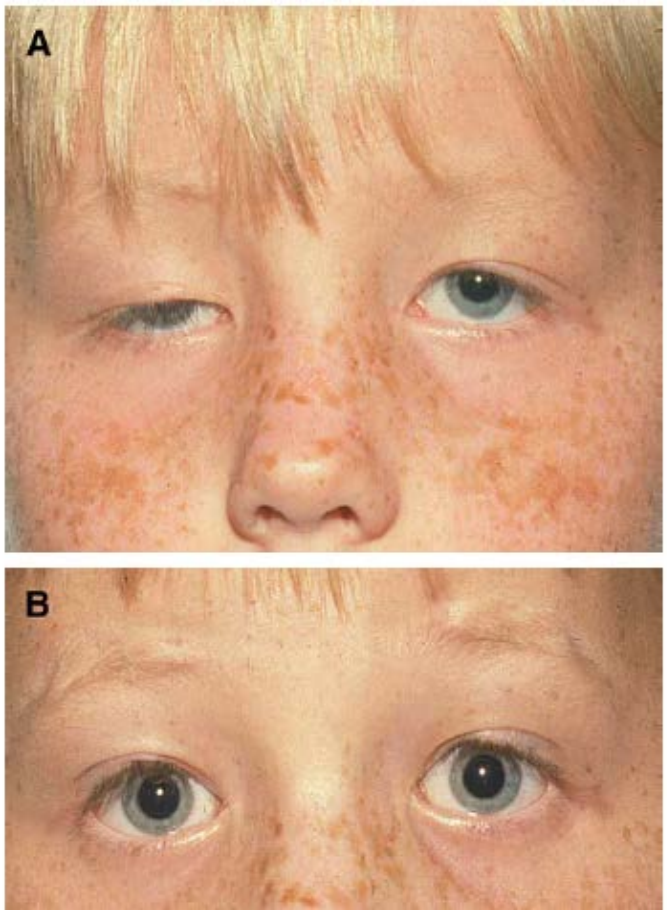

Figure 8: Efficacy of performing frontalis suspension procedure with a fascia lata sling on a 5-year-old patient suffering congenital ptosis in right eye: (A) before frontalis suspension surgery, (B) after frontalis suspension surgery – picture source: Edmonson et al. [17]

Frontalis suspension failure and recurrence of Ptosis

Some of the common complications associated with frontalis suspension are infection, extrusion, and granuloma formation. Moreover, one of the sever problems and complications that are associated with frontalis suspension is ptosis recurrence after the surgery [5], [41]. Numerous researchers believe that sooner or later all the congenital cases that have been treated with frontalis suspension will recur. Several authors have reported the rate of ptosis recurrence after the frontalis

suspension surgery. In some studies and for some suspension materials the recurrence rate have been even reported as high as 100%. [41][42][43][33][44]

Figure 9: Two of the common complications of frontalis suspension surgery; (A) Infection, (B) Granoluma formation – picture adapted from Ben Simon et al., The Open Ophthalmology Journal, 2010, Vol. 4. [5]

The time to recurrence that is mentioned in different studies was not equal between materials and between studies. Different patient samples, sample sizes, and surgeons could be a reason for these differences. For example, Ben Simon et al. have reported an average of 12.2, 13, and 16.5 months to recurrence respectively in autogenous fascia lata, silicone, and nylon. They observed ptosis recurrences in 42 cases (25.6%) out of 164 cases after a mean 12 months from first surgery. They reoperated 26 of the eyelids. [5]

Hypothesis and Research Plan

The reason for frequent recurrence of ptosis after frontalis suspension is not yet understood very well. There are numerous cases that ptosis recurs in the patient eye after a few years while no infection, granuloma formation, rejection of the sling by the body, or other complications are discernable. This issue becomes more interesting especially considering that different recurrence rates have been reported for different materials by different researchers [5], [33], [41], [43], [45]–[48]. Therefore, researchers have proposed and investigated that the sling material choice might be a factor influencing the recurrence rate. Several studies have retroactively investigated the effect of suture material on ptosis recurrence [5], [41], [44]. However, as no prospective study has been done on this issue, the effect of the material on the recurrence could not be singled out.

An average person blinks once every five seconds. Therefore, an eye blinks on average about 15,000 times during a normal day spanning 16 hours. This can vary depending on the amount of time a person is awake and can be as high as 40,000 times every 24 hours [49], [50]. Annually, a sling may experience tens of millions of episodes of loading and unloading. Some slings have ceased to function after many cycles of loading and have had to be replaced even though they were still intact. Possibly, the sling changed somehow in these cases such that it could not support the eyelid to the extent that it did when it was implanted [44]. Therefore, it is reasonable to hypothesize that possible changes in mechanical properties of these slings under repetitive loading from eye blinking could cause changes in the implanted sling material that leads to ptosis recurrence after some time.

In order to investigate this issue in more depth, we have developed different experimental setups to study the frontalis suspension sling materials under physiologically relevant cyclic loading conditions. In the following chapters, we first discuss previous studies performed about mechanical properties of different sling or suture material in Chapter 2. Following that, we will discuss the development of our different experimental setups for study of sling materials alongside our experimental results and analysis in Chapters 3, 4, and 5. Finally, we conclude this dissertation in Chapter 6 by summarizing the results and proposing the future work.

Chapter 2

Literature Review on Previous Studies about Mechanical Properties of Sutures and Slings

Sutures and synthetic slings

Sutures are basically used to hold body tissue together after injury or surgery. The first sutures were made from biological materials, such as catgut suture or silk. However, most current sutures are synthetic. Suture treads could be made of various materials. They can be either absorbable or non-absorbable after implantation to the body. Absorbable suture materials are capable of being absorbed by living mammalian tissue, but maybe treated to modify their resistance to absorption. Some examples of absorbable suture materials are polyglycolic acid, polylactic acid, monocryl and polydioxanone. Non-absorbable suture materials which are basically resistant to the action of living mammalian tissue maybe in either monofilament or multifilament form. Some examples of non-absorbable suture materials are nylon, polyester, polyvinylidene fluoride and polypropylene.[51] [52]

Surgical Sutures are available in a number of sizes. They are classified into different sizes based on their thread diameter. Classification of sutures into various sizes by United States Pharmacopeia (U.S.P.) is widely accepted across the world. Conversely, certain European countries use the Metric system of classification of sutures based on the suture size. This classification assists manufacturers across the world to implement uniform standards and also benefits surgeons in selecting and ordering the right size of suture essential for a specific procedure. The following table provides the U.S.P. and metric suture sizes chart for the diameter range for synthetic sutures. [53]

Table 1: Suture Sizes Chart

U.S.P. Size	Synthetic Sutures	
	Metric Size	Diameter Range (mm)
# 7	9	0.900 - 0.999
# 6	8	0.800 - 0.899
# 5	7	0.700 - 0.799
# 4	6	0.600 - 0.699
# 3	6	0.600 - 0.699
# 2	5	0.500 - 0.599
# 1	4	0.400 - 0.499
# 0	3.5	0.350 - 0.399
# 2-0	3	0.300 - 0.339
# 3-0	2	0.200 - 0.249
# 4-0	1.5	0.150 - 0.199
# 5-0	1	0.100 - 0.149
# 6-0	0.7	0.070 - 0.099
# 7-0	0.5	0.050 - 0.069
# 8-0	0.4	0.040 - 0.049
# 9-0	0.3	0.030 - 0.039
# 10-0	0.2	0.020 - 0.029

Studies on mechanical properties of sutures

In 1976, Holmlund published his investigations about the stress-strain relationship, the stress-relaxation and the irreversible elongation of different suture materials [54]. In this study, an Instron table model machine was used to test various 3-0 sutures including nylon, prolene, supramid, catgut, mersillene, silk, linen, and steel. It was found that the distensibility (stretchability) of the sutures with the same size but different material varied significantly. Most sutures were found to be mainly elastic but some sutures were elastic when a moderate load was applied and plastic when the load increased. Some sutures, especially Prolene, were plastic also when moderate load was applied. His experiments also pointed out large differences in the stress strain relations between the different nylon sutures of Astra, Ethilon, and Ethicon type. Different suture material elastic properties investigated by Holmlund are mentioned in Table 2.

Table 2: Different suture material elastic properties. In this table *e* is basically the increase in length per unit length (i.e. strain) and therefore, $\frac{1}{e}$ is a measure of modulus of elasticity; Elong.^{EL} is the elongation % at the elastic limit; and Elong.^{YP} is the elongation % at the Yield Point. Table is extracted from Holmlund et al. [54].

Suture Material (3-0)	$\frac{1}{e}$	Elastic Limit (Kp)	Elong.^{EL} (%)	Yield Point (Kp)	Elong.^{YP} (%)
Ethilon blue	52	1.3	24	1.8	43
Ethilon black	57	1.7	28	2.4	54
Nylon (Astra)	59	2.1	35	2.4	45
Prolene	80	1.0	15	1.8	55
Nylon (Ethicon)	81	1.5	18	2.1	35
Supramid	110	2.2	20	2.4	27
Catgut Chromic	110	1.0	9	2.4	24
Catgut Plain	110	1.0	9	2.5	25
Dexon	140	1.0	7	2.3	24
Ethiflex (Ethicon)	170	4.1	20	4.1	20
Dacron (D & G)	190	3.1	13	3.3	19
Tevdek (SSC)	190	3.1	13	3.3	17
Mersilene (Ethicon)	230	3.4	17	3.4	17
Silk (Astra)	240	1.0	4	2.2	22
Silk (SSC)	240	1.0	4	2.1	9
Silk (Ethicon)	280	1.0	3	2.0	16
Silk (D & G)	420	1.0	2	2.1	11
Linen (Ethicon)	570	3.4	3	3.4	3
Steel (Polyfil)	850	1.5	2	2.7	30
Steel (Monofil)	1200	2.1	2	3.6	65

When a continuous stress is applied, all suture materials show a viscoelastic behavior. This means that once a suture material is stretched and then held at the new length, tension gradually falls. This phenomenon is known as **stress relaxation**. Similarly when constant or repeated loadings are applied to the material, it will increase in length immediately and then continue extending until it reaches a state of equilibrium. This phenomenon is known as **creep** [55]. Under repeated loading, this phenomenon can also be called strain ratcheting. Due to the plastic behavior and the creep phenomenon in the suture, its length increases with the intensity and duration of the stress applied. One part of this elongation, the irreversible elongation, remains even when the load is removed. Irreversible elongation of different suture materials after single and multiple loadings and stress relaxation of different types of suture materials as reported by Holmlund are listed in Table 3, and Table 4 respectively.

Table 3: Irreversible elongation of different suture materials after repeated stress. Table is extracted from Holmlund et al. [54].

Suture Material 3-0	Number of Loadings					
	1	30	60	120	240	360
Silk (Ethicon)	2	3	3	3	—	—
Catgut (Chromic)	2	4	5	5	—	—
Nylon (SSC)	4	7	8	8	8	8
Ethilon blue (Ethicon)	7	12	14	14	15	15
Prolene (Ethicon)	14	18	20	24	27	30
Ethiflex (Ethicon)	2	3	3	4	—	—
Suturamid (Ethicon)	3	3	5	6	6	—
Steel monofilament	2	4	4	4	—	—
Dexon	4	7	8	8	—	—

Load 1.5 kp; elongation in per cent of initial length.

Table 4: Stress Relaxation of different types of suture materials. Table is extracted from Holmlund et al. [54].

Suture Material 3-0	Initial Stress (kp)	Remaining Tension (kp) after 1′	3′	60′	16 h	Irreversible Elongation after 16 h (%)
Silk (Ethicon)	1.5	1.2	1.1	1.0	1.0	4
Catgut (Chromic)	1.5	1.3	1.2	1.1	1.0	3
Dexon (Davis & Geck)	1.5	1.3	1.2	1.1	1.0	7
Nylon (SSC)	1.5	1.2	1.2	1.1	1.1	7
Ethilon blue (Ethicon)	1.5	1.2	1.1	1.1	1.1	12
Prolene (Ethicon)	1.5	1.1	0.9	0.6	0.3	15
Ethiflex (Ethicon)	1.5	1.2	1.2	1.1	1.1	3
Suturamid (Ethicon)	1.5	1.2	1.2	1.1	1.1	5
Linen (Ethicon)	1.5	1.2	1.1	1.0	0.9	1
Steel (monofil)	1.5	1.2	1.2	1.1	1.1	2

Nilsson has published a series of papers related to the mechanical properties of Prolene (polypropylene), and Ethilon (nylon) sutures (sizes 2-0 and 6-0). In these reports, the terminology used to describe the mechanical properties of the materials for suturing were somehow confusing and different from the standard terminology used in material science. Therefore, here we first provide the definitions and measuring units of the parameters considered in his studies: the *cross-sectional area* was expressed as the weight per length unit (mg per mm); the *breaking load, maximum load (F_{max})* is the force (in Newtons) needed to rupture the sample; the *tensile strength (maximum stress) (δ_{max})* is the breaking load per cross-sectional area (Newtons per mg per mm); The *energy absorption (load-strain area (L/S)* or *stress-strain area (S/S)* is the amount of energy used to rupture the specimen or the material. It is determined for the specimen as the area under the load-strain curve (in Newtons) or for the material as the area under the stress-strain curve (in Newtons per mg per mm); the *elastic stiffness* is an expression of the stiffness of the specimen or the material. It is defined as the steepest part of the load-strain curve (*tan α S/S* in Newtons per mg per mm); the *plasticity* is the permanent deformation expressed in percent of the original length when successive loadings to 1/3, 1/2, 2/3 and 8/9 of F_{max} value are applied. In fact, correction of the cross-sectional area to weight per length unit in these study series is sufficient to compare

differently sized threads of the same material. However, this correction excludes any direct comparison between the suture materials as far as their physical characteristics are concerned.

Nilsson showed that the physical characteristics of the materials in Prolene and Ethilon vary with the size of the threads (see Table 5) in his first study about suture material properties [56]. Interestingly, this investigation revealed that the difference between two different suture sizes of 2-0 and 6-0 of the same suture material was mainly due to the characteristics of the materials and not just due to the manufacturing processing (polymerization) used for different thread sizes.

Table 5: Results of testing the tensile properties of Prolene and Ethilon sutures (sizes 2-0 and 6-0) as reported by Nilsson [56]

USP size	Suture materials	F_{max} (N)	δ_{max} (N · mm · mg^{-1})	Area L/S (N)	Area S/S (N · mm · mg^{-1})	ε_{max}	tan α L/S (N)	tan α S/S (N · mm · mg^{-1})
6–0	Prolene®	6.12 ±0.09	842.81 ±16.20	128.95 ±2.35	17 749.19 ±381.78	0.38 ±0.01	20.06 ±0.45	2 763.29 ±89.49
2–0	Prolene®	49.40 ±0.85	717.40 ±27.60	2 086.05 ±79.03	30 387.05 ±1 924.31	0.75 ±0.02	96.70 ±1.56	1 402.09 ±39.64
6–0	Ethilon®	6.68 ±0.13	964.88 ±40.02	112.00 ±8.53	16 095.97 ±1 065.74	0.35 ±0.02	28.73 ±1.16	4 165.65 ±269.88
2–0	Ethilon®	59.14 ±1.96	772.67 ±27.12	1 569.29 ±95.86	20 437.21 ±1 035.16	0.62 ±0.02	154.69 ±6.80	2 027.54 ±124.73

In another study, Nilsson showed that the mechanical characteristics of Prolene (polypropylene) and Ethilon (nylon) sutures depend on the strain rate. Furthermore, Nilsson investigated the influence of mechanical loading and degradation on the mechanical characteristics of Prolene and Ethilon [57]. To do so, Prolene and Ethilon sutures were implanted in rabbit abdominal wounds and muscle pockets followed by dissection 21 days after implantation. This investigation showed that sutures experience in vivo changes in their mechanical characteristics partially due to

mechanical loading, and partially to the degradation. The changes were dissimilar in polypropylene and nylon and depended on the size of the suture.

In 1994, Greenwald et al. published a paper reporting their studies on the material properties of ten 2-0 suture materials. The tension in these sutures were evaluated before and again after 6 weeks incubation in rats. Based on the experimental results, they reported stress-strain curves, strength, toughness, strain at rupture, and elastic modulus of these sutures. The tested sutures in this study included Vicryl [poly(glycolide-lactide)], Dexon (polyglycolic acid), Ethibond (polyester), silk, plain gut, chromic gut, Maxon (poly-glyconate), PDS (polydioxanone), nylon, and Prolene (polypropylene). Their results revealed that, before incubation, PDS and Maxon were the strongest and toughest while silk demonstrated the least strength and toughness. Strength, and toughness decreased in all of the sutures over time in vivo with the exception of braided polyester (Ethibond), which remained stable. Interestingly, Vicryl, Dexon, and gut sutures were absorbed to the point that they could not be tested after 6 weeks in vivo [58].

In another study, Vizesi et al. performed creep and relaxation tests in tension on different 4-0 sutures commonly used for hand tendon repair plastic surgeries. The tested materials included monofilament polypropylene (Prolene), monofilament nylon (Ethilon), and braided polyester fiber (Ticron). It was found that Ticron was the stiffest suture at both room and body temperature, followed by Prolene and Ethilon. Both Prolene and Ethilon exhibited reduced stiffness at body temperature. Prolene was the only material to show temperature effects in creep and relaxation. It also unveiled larger relaxation and creep ratios than Ethilon and Ticron [59].

Mechanical properties of frontalis suspension synthetic sling materials

With respect to frontalis suspension application, Kown et al. have also started to study the mechanical properties of some commonly-used synthetic frontalis suspension materials—namely, monofilament polypropylene (Prolene), sheathed braided polyamide (Supramid Extra II), silicone frontalis suspension rod (Visitec Seiff frontalis suspension set), woven polyester (Mersilene mesh), and expanded polytetrafluoroethylene (ePTFE) (Ptose-Up). Supramid Extra II is a suture that is formed by twisting nylon filaments into a thicker fiber. Mersilene mesh sling is formed by inter-weaving polyester fibers into a mesh.

In their first paper on this topic [60], they focused on investigation of some synthetic materials used for frontalis suspension under static tensile loading conditions (see Figure 10). They tested each aforementioned material under a single tensile loading to the failure of the material, at three different displacement rates (1, 750 and 1500 mm/min).

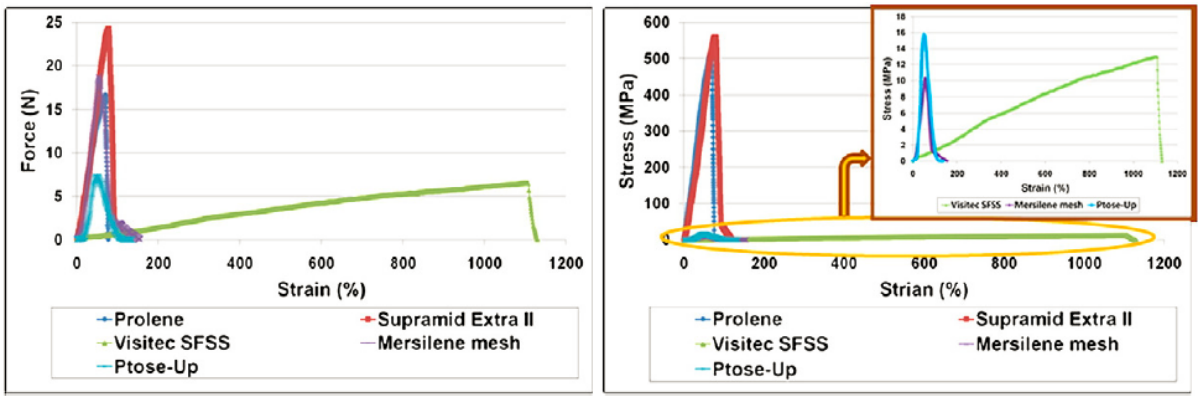

Figure 10: Results of the tensile test at 1500 mm/min strain rate of common synthetic frontalis suspension materials - this diagram is extracted from Kwon et al., Journal of Material Science and Engineering C [60]

They reported that all the materials mentioned above presented elastic–plastic tensile stress-strain behavior with considerable differences in elastic modulus, ultimate tensile strength, elastic limit and work of fracture. Figure 11 shows the summary of the key mechanical properties of the investigated by Kwon et al. frontalis suspension slings under static tensile loading. Based on these results, it was proposed that silicone rod might be the most suitable synthetic frontalis suspension sling since it not only shows a low elastic modulus and stiffness leading to lower possibility of "cheese-wiring" effect through the soft tissue underneath, but also its reasonable work of fracture and elastic limit are such that the sling will not break under the loadings when implanted as a sling in the body.

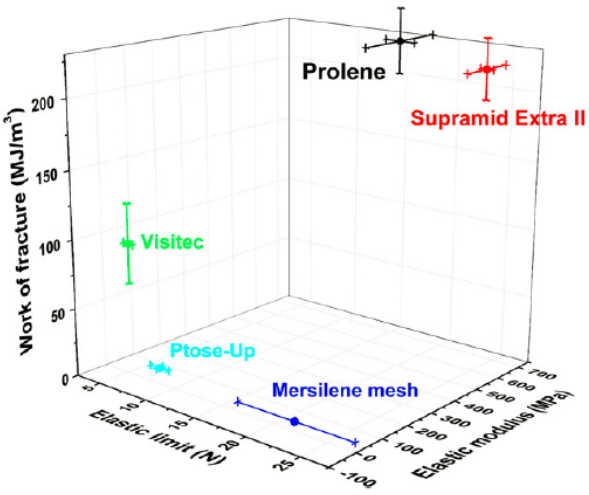

Figure 11: Comparison of elastic limit, elastic modulus, and work of fracture of different frontalis suspension materials investigated under static loading by Kwon et al. – this diagram is extracted from Kwon et al., Journal of Material Science and Engineering C [60]

In their second paper on this topic, Kwon et al. focused on testing various synthetic brow-suspension materials (Prolene, Supramid Extra II, Silicone rods (Visitec Seiff frontalis suspension set) and Mersilene mesh) under dynamic loading in room temperature [61]. They also reported

stress relaxation and creep behavior for all of the aforementioned frontalis suspension materials. All the materials except Prolene exhibited a similar relaxation trend by reaching the steady state at around 10 minutes of the relaxation time. The significantly different time-dependent response of Prolene was also confirmed by creep tests.

Table 6 describes the fatigue test protocol Kwon et al. used. Uniaxial tensile fatigue tests demonstrated extremely different time-dependent response amongst the different materials as shown in Figure 12.

Table 6: Uniaxial displacement –controlled fatigue test protocol as used by Kwon et al. [61] to investigate the synthetic frontalis suspension sling materials under cyclic loading condition

Segment number	Process
1	Position hold at 0 mm (=0% strain) for 1 s
2	Ramping to 1.5 mm (=15% strain) at 1 mm/s
3	Displacement-controlled sinusoidal oscillation between 0 mm and 1.5 mm (i.e. 0–15% strain with mean strain of 7.5%) at 6.5 Hz for 100,000 cycles
4	Position hold for 1 s

As the authors claim, the fatigue machine they used was operated to its limit, thereby generating some artifacts in the data; these artifacts explain some of the gaps between data points on the peak force vs. cycle number graph below.

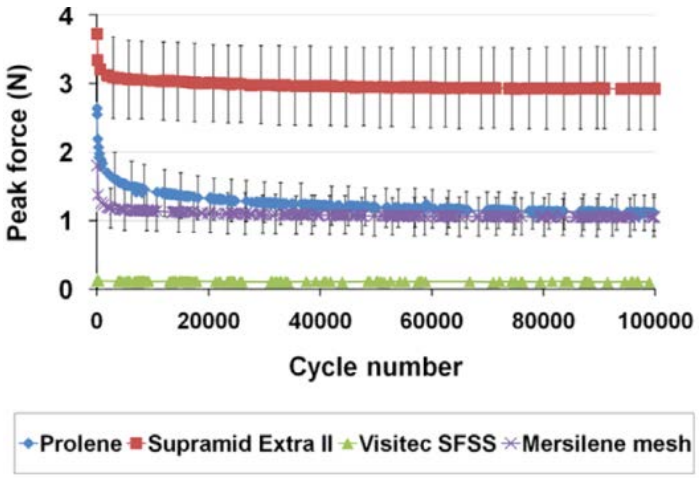

Figure 12: Fatigue test results (average peak force vs. cycle number) in four different synthetic frontalis suspension sling materials as reported by Kwon et al. in J Mech Behav Biomed Mater [61]

Fascia Lata

The fascial system is an integral part of the musculoskeletal system that is responsible for the structural integrity of the organism, warranting its strength and the ability to react efficiently to external and internal mechanical stimuli. It is a three-dimensional network of connective tissue distributed ubiquitously throughout the body, surrounding muscles, bones, internal organs, nerves, vessels, and other structures. The connective tissue forming fascia is mostly made of collagen fibers and, to a lower degree, of elastic fibers. The high collagen content ensures its strength and flexibility. The collagen fibers are arranged in the fascia in a spatial network that the cellular elements are suspended [62], [63].

Fascia lata is the deep fascia of the thigh that encloses the thigh muscle. It is an anisotropic biomaterial, composed of a bilayer of tendon fascicles. The deep fascicles are approximately parallel and oriented in the proximal-distal direction along the primary axis of mechanical loading, whereas the overlaying fascicles follow an oblique orientation relative to the deep layer [64].

Autograft and allograft fascia lata has been used in the surgical treatment of soft tissue repairs or reconstructions by orthopedists [65] , ophthalmologists [66] and urogynecologists [67]. Using allograft fascia lata in relevant surgeries eliminates the morbidity associated with harvesting the autograft tissue.

Processed fascia lata

Processing techniques used in sterilization and storage of allograft fascia lata is varied. Fascial allografts are usually obtained under sterile conditions or secondarily sterilized and then freeze dried (lyophilized) for storage. Lyophilization or freeze drying is a process in which water is removed from a graft after it is frozen and placed under a vacuum, allowing the ice to change directly from solid to vapor without passing through a liquid phase [68]. The solvent-dehydrated fascia lata offers an alternative method of preparation using acetone to slowly dehydrate allograft material in an ambient air-drying chamber. Freeze-drying and deep freezing reduce viral titers, but do not guarantee complete suppression [68], [69].

Acellularization and/or antibiotic soak treatment, together with lyophilization, are some other standard allograft tissue processing methods. Acellularization treatment is intended to disrupt cells and remove water-soluble cellular proteins to reduce antigenicity. Acellularization may also enhance host cell infiltration with phenotypically appropriate cells and prevent possible transmission of infectious genomic vectors [70].

Previous studies on mechanical properties of fascia lata

Some basic studies of the biomechanical properties of fresh and processed fascia lata have been done previously. Gratz was one of the first who studied the mechanical properties of fascia lata. He emphasized on the difficulties of mechanically testing this slippery and soft tissue and showed that fascia lata graft mechanical properties depend on its longitudinal fiber alignment, cross-sectional area, and donor's activity level and age [71]. He reported tensile strength of around 7860 lbs. per sq. in. (54.2 Mpa) for fascia lata. In one of the first few studies on fascia lata mechanical properties by Gratz, the graphs of tensile strength and elasticity for living human fascia lata and dead (prepared) human fascia lata was provided (see Figure 13).

The curves in the Figure 13 graphs show the reaction of living (fresh) and dead (prepared) fascia lata to varying degrees of tension; the curve on the right side of each graph shows the corresponding elasticity. As tension is applied an elongation takes place (*0* to *A*), then the material stiffens *(A* to *B)* and finally relaxes again (after *B*). Upon releasing the tension the test piece returns nearly but not completely to its original length. When subjected to tension greater than before, the same cycle is repeated except that the material is slightly stiffer and less elastic. Finally, when sufficient tension is applied, the material is destroyed [71].

The relation of above findings to the structure of fascia lata can be explained considering the previous microscopic studies performed on its structure. Fascia lata consists of a mass of very thick parallel fibers which runs a straight or slightly wavy course. Between these fibers are scattered a small number of connective tissue corpuscles (tendon cells). The fibers are gathered into bundles which are separated by a small amount of areolar tissue. Areolar tissue is a common type of loose

connective tissue that its fibers are far enough spread out to leave plenty of open space for interstitial fluid in between. Alveolar tissue is strong enough to bind different tissue types together, yet soft enough to provide flexibility and cushioning. It also serves as a reservoir of water and salts for surrounding tissues. The parallel arrangement of heavy fiber fascia gives it great strength in one direction, i.e. in the direction in which it is normally subjected to strain [72].

A probable explanation of the mechanical behavior of fascia lata explained above is in successive adjustments of its composing materials to the tension applied. The areolar tissue cells, being weaker than the fibers, are the first to break down, leaving the tension to be resisted by the stronger fibrous material. With an increase in the tension applied, the fibers begin to separate from the tendon cells. The final rupture of the material occurs with the pulling apart of the fibers one from the other.

The fibers also behave as the elastic elements. The elasticity is interfered with to some extent by the areolar tissue, especially after it is broken down by excessive stretching. In spite of this, however, the elasticity (capacity to return to original dimensions) of the material, under the limits of maximum safe stress, is above 91% as shown by the elasticity curves in Figure 13. The graphs in Figure 13.B depict the tensile strength and elasticity curves of dead (prepared) fascia lata. It can be noted that the elasticity of the prepared fascia lata does not compare favorably with the living fascia lata.

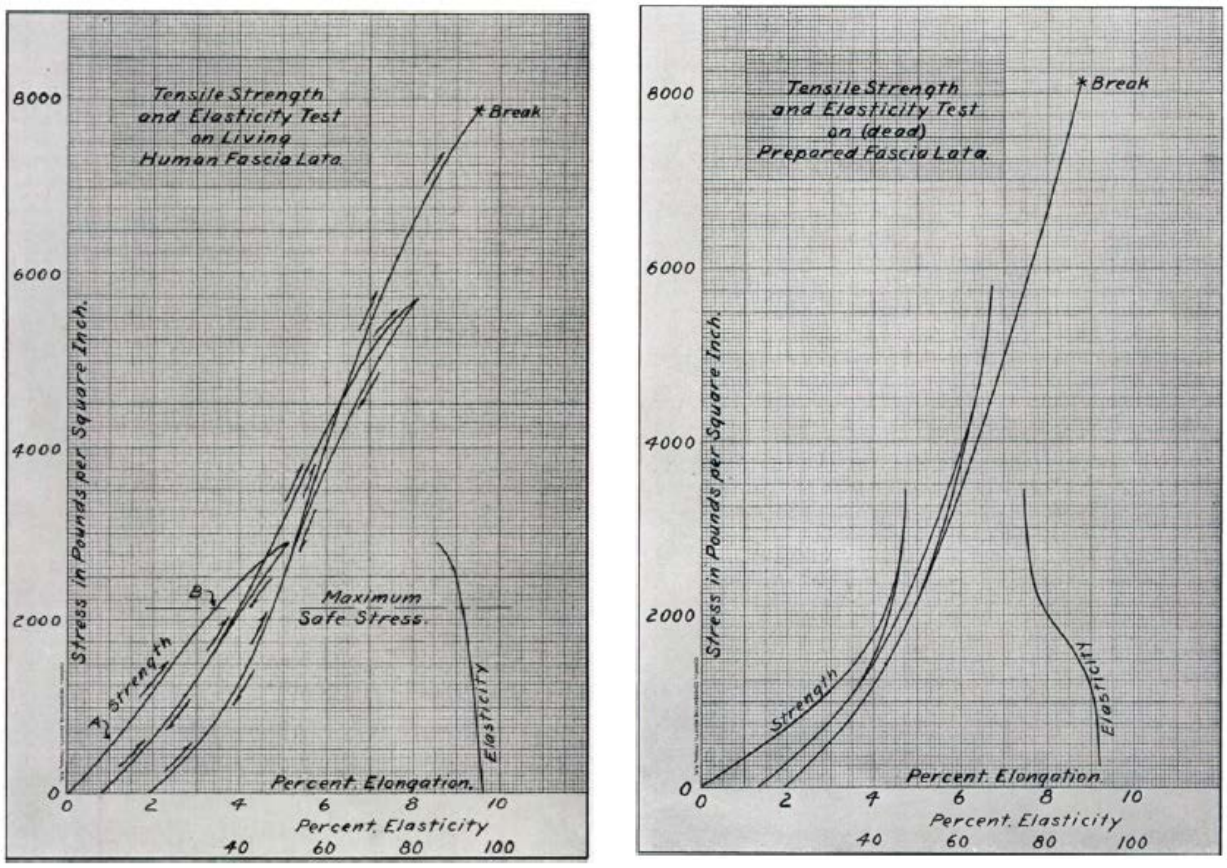

(A) (B)

Figure 13: Tensile strength and elasticity graphs for (A) Living human fascia lata, and (B) dead (prepared) human fascial lata as reported by Gratz. Picture Source: Gratz, The Journal of Bone & Joint Surgery, 1931 [71]

Techniques of procurement, sterilization, and storage processing of fascial allografts are varied, and the methods used have been questioned as a source of alteration in the graft's initial mechanical properties in vivo function [73]. While early investigation by Thomas and Gresham found no significant differences in tensile strength between fresh, frozen, and freeze-dried fascia lata specimens, other studies reported different results. For example, Hinton et al. reported significantly

higher stiffness, higher maximum load to failure, and higher maximum load per unit width of graft with the solvent-dried as opposed to the freeze-dried fascia lata (see Table 7) [74].

Table 7: Mechanical properties of solvent-dehydrated versus freeze0dried fascia as reported in Hinton et al. – Table extracted from [74]

	Mechanical properties (mean ± SD)				
Allograft	Maximum load[a] (N)	Maixmum load/ graft width[a] (N/mm)	Stiffness[a] (N/mm)	Maximum stress (N/mm^2)	Maximum strain (% strain)
Solvent-dehydrated	315.9 ± 52.5	31.6 ± 5.3	188.2 ± 35.9	53.9 ± 6.9	22.8 ± 3.3
Freeze-dried	262.1 ± 66.1	26.2 ± 6.6	158.3 ± 40.8	55.6 ± 8.8	23.6 ± 4.1

[a] Statistically different: $P < 0.05$.

In another study, Derwin et al. assessed the mechanical, chemical and biophyscial properties of human fascia lata as a scaffold for soft tissue repair and tissue engineering applications. Linear modulus of fresh fascia lata (FRESH), fascia lata treated by antibody (ABX), and fascia lata first acellularized and then treated by antibody (ACELL+ABX) were reported by them as 389 ± 189 MPa, 532 ± 106 MPa, 440 ± 326 MPa, respectively. Figure 14 that is extracted from [75] shows the effect of antibiotic soak treatment (ABX) and acellularization followed by antibiotic soak treatment (ACELL+ABX) on the mechanical properties of the fascia lata patch.

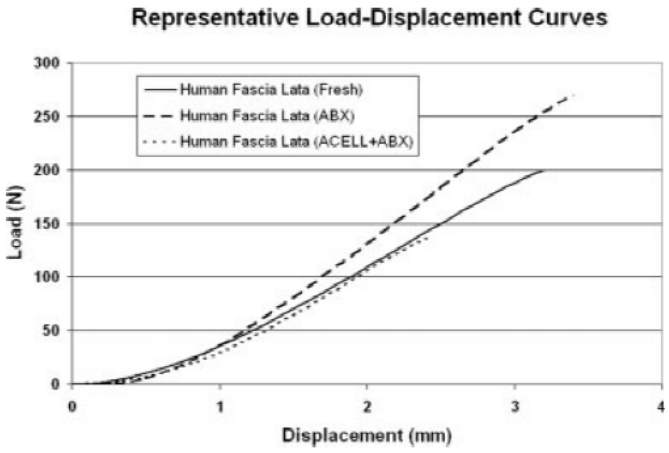

Variable and Treatment	Median (Range)	Mean (Std)
Linear stiffness[a] (N/mm)		
Fresh, $n = 10$	82.8 (61.8, 105.8)	85.1 (15.4)
ABX, $n = 10$	99.2 (71.4, 121.5)	98.2 (16.2)
ACELL+ABX, $n = 10$	79.1 (7.0, 124.0)	71.2 (38.9)
Linear modulus[b] (MPa)		
Fresh, $n = 9$	392 (83, 702)	389 (189)
ABX, $n = 8$	523 (337, 654)	532 (106)
ACELL+ABX, $n = 10$	458 (38, 1146)	440 (326)

Figure 14: Biomechanical properties of fresh and processed human fascia lata as reported by Derwin et al. [75]

Derwin et al. study data demonstrate that tissue processing does not significantly change the stiffness or modulus of fascia lata. While this result is supported by Thomas and Gresham study results [73], it is not supporting the Hinton et al. study results [74].

Furthermore, the data provided by Derwin et al. can give a good approximation of the effect of where the fascia lata sample is harvested from as well as different processes that are performed on it on the properties of the sample. For instance, as a reference, Table 8 that is basically extracted from [75] shows how 6×12 cm^2 fascia lata samples from different regions with respect to the iliotibial tract have different thickness and stiffness.

Table 8: Effect of location on thickness and stiffness of fascia lata samples as mentioned in Derwin et al. – Table extracted from [75]

Measurement	Location	Mean (SD)	*p*-Value
Thickness (mm)	All Regions	0.55 (0.15)	0.53
	Distal 1	0.60 (0.25)	
	Distal 2	0.52 (0.09)	
	Proximal 1	0.55 (0.13)	
	Proximal 2	0.56 (0.10)	
Stiffness (N/mm)	All Regions	85.1 (22.2)	0.97
	Distal 1	86.6 (18.1)	
	Distal 2	82.7 (27.5)	
	Proximal 1	86.2 (27.9)	
	Proximal 2	84.7 (16.4)	

These data were derived from samples taken from four quadrants of a 6 × 12 cm^2 region of 10 human fascia lata. The *p*-value is from an *F*-test of differences between regions.

Finally, in a paper published by Aurora et al. about a reinforced fascia patch for rotator cuff repair, they have described a method for characterizing mechanical properties of fascia patches. In these patches, fascia was reinforced by stitching with PLLA or PLLA/PGA polymer braids. In their study, tensile failure and fatigue tests were done on these reinforced 5×5 cm^2 fascia patches. The mode of failure here was breaking of the braid combined with slipping of the braid through the fascia matrix [76]. Since this study was established for fascia patches reinforced with PLLA/PGA polymer braids, not plain fascia samples, the results could not be referenced for fascia mechanical properties. Hence, the drawn mechanical property behavior in this study are more related to the hybrid of fascia and polymer braids not just the fascia nor the polymer braids. However, the methods and results in this study are insightful towards one of the goals of our research trust, i.e. study of fascia lata under physiological relevant conditions for the slings used in frontalis suspension.

In conclusion, several studies have been done on the mechanical properties of sutures under static and dynamic loading. In these studies, some of the sutures or possible sling materials have been investigated whether in room temperature or implanted in animal models. Some of these sutures have application in frontalis suspension procedure. Also, just a couple of studies have been previously done on the sutures and synthetic slings specifically used for frontalis suspension procedure. One of these studies has just focused on static loading condition, while the other one has considered the dynamic loading and fatigue condition. Also, several studies have been done on the mechanical properties of fascia lata. The focus of none of these studies have been on investigation under physiologically relevant condition of the fascia lata that is used specifically in frontalis suspension surgery.

Chapter 3

Study of Incidence of Plastic Elongation in Frontalis Suspension Slings

In this chapter, we discuss our hypothesis about a possible cause for ptosis recurrence after a few years following frontalis suspension surgery. Afterwards, we discuss the method and the first experimental setup we developed and used to investigate this hypothesis. Finally, the results of the experiments performed with the aforementioned developed setup are presented and a discussion about the results is provided.

Hypothesis

We hypothesize that the failure and hence recurrence of ptosis after the surgery is due to gradual cumulative permanent strain (strain ratcheting) resulting from repeated loading and unloading of frontalis suspension sling material each time the eye blinks that is associated with structural changes within the sling material.

The present work was the first evaluation to our knowledge of the incidence of fatigue induced plastic elongation, and other related physical changes, in common materials used in frontalis suspension blepharoptosis repair. In order to investigate this hypothesis, we first developed a

proof-of-concept setup and experimental method to test different sling materials under fatigue conditions in air and in a saline solution to simulate an interstitial environment and to counteract dehydration effects for the biologic materials.

Background

A few terms used in material science are defined in the following which may be helpful in reading the subsequent materials and methods chapter.

Plastic deformation

A stress that is applied to a structural material will generally cause it to change shape. This change in shape is called deformation. A temporary shape change that is self-reversing after the force is removed, so that the object returns to its original shape, is called *elastic* deformation. In other words, elastic deformation is a change in shape of a material at low stress that is recoverable after the stress is removed. When the stress is sufficient to permanently deform the material, the remains strain after unloading is called *plastic (permanent)* deformation.

Fatigue

Fatigue as a materials science term is the weakening and progressive structural damage of a material caused by repeatedly applied loads (cyclic loading). The nominal maximum stress values that cause such damage may be much less than the strength of the material typically quoted as the ultimate tensile stress limit, or the yield stress limit.

Strain ratchetting

Consider a sling specimen as shown schematically in Figure 15. If the sling is stretched by a force $F = F_1$ that causes a stress less than its yield stress limit, it elongates predominantly elastically for an amount of δ. If the sling specimen gets unloaded, it appears to return to its original length because the plastic strain that occurs is insignificantly small. But if the sling specimen is loaded and unloaded repeatedly (fatigued) for a large number of cycles N, it can become significantly elongated permanently (plastically), equal to δ_p in Figure 1. This gradual cumulative permanent strain is called strain ratchetting [77].

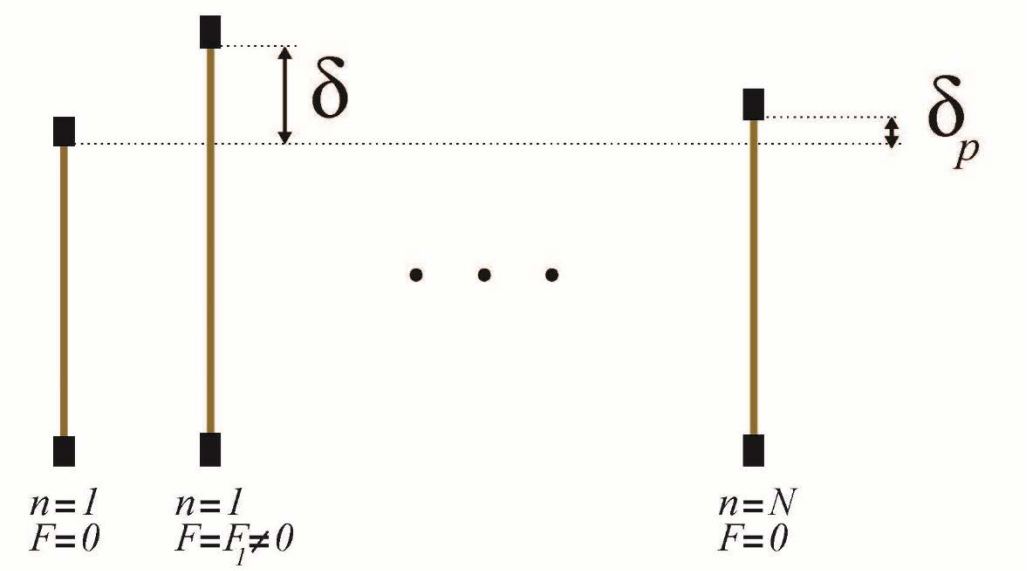

Figure 15: The concepts of strain ratchetting occurrence in a sling under cyclic loading (fatigue) condition

Materials and Methods

A novel mechanical test system was devised to study the incidence of plastic (permanent) elongation due to applied cyclic strain in the sling specimens. In this test system, the sling specimen

with a length of $\boldsymbol{l_0 = 100\ mm}$, which is the average length commonly employed for single rhomboid frontalis suspension [78], is attached to a loading system via two grips (

Figure 16).

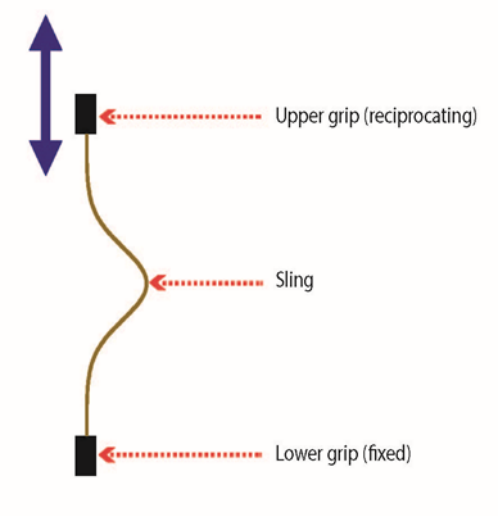

Figure 16: Schematic of the experimental setup

The lower grip was fixed, while the upper grip underwent a linear reciprocating movement with a fixed span of $2a$ and frequency of f. Therefore, the position of the upper grip, y, can be described by the following, assuming the origin is at the lowest possible position of the upper grip:

$$y = a\,(1 + \cos(2\pi f t\ +\ \pi))$$

Thus, the speed of the upper grip can be described as:

$$v = \frac{dy}{dt} = -2\pi f a \sin(2\pi f t + \pi)$$

In the present study, the parameters a and f were set such that the maximum speed of the upper grip, that is equal to the maximum speed of the moving end of the sling specimen, is the same as

the maximum speed of the palpebral end of the implanted sling in patients that underwent frontalis suspension procedure, i.e. equal to the peak voluntary blinking speed reported in the literature [79].

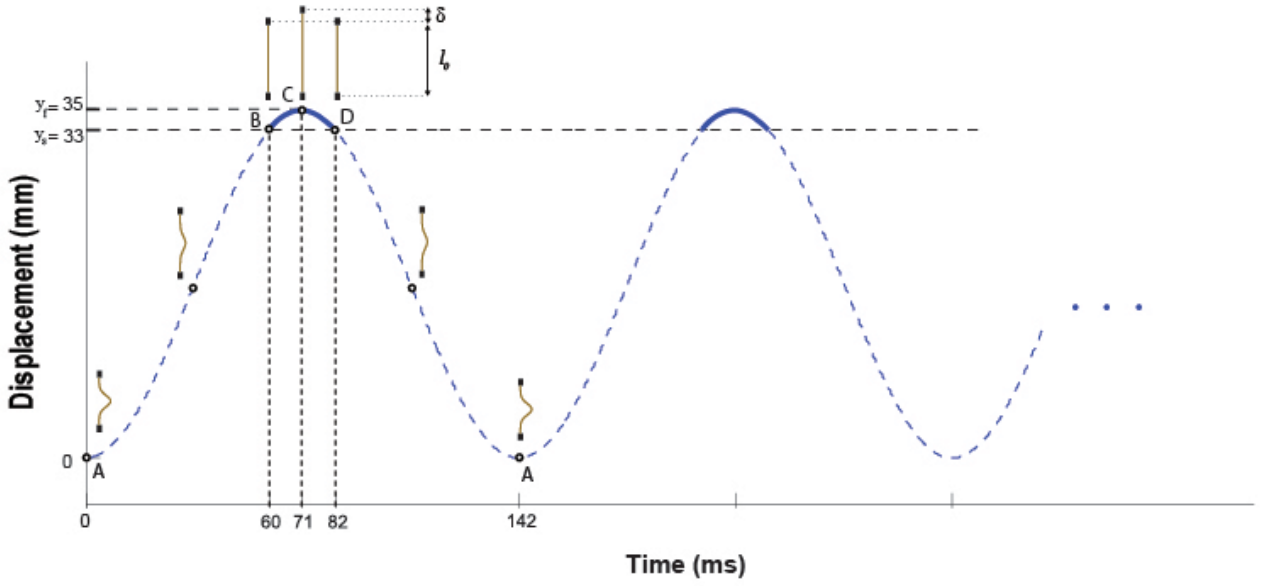

Figure 17: Diagram of the experimental setup upper grip displacement

As depicted in Figure 17, each cycle of the test takes $\frac{1}{7\text{ Hz}} \cong 142$ ms by choosing $f = 7$ Hz. By choosing the span of the upper grip, $2a = 35$ mm, the specimen length, $l_0 = 100$ mm, and maximum occurred stretch in the sample, $\delta = 2$ mm, we will have a situation in which out of the $142\ ms$ time length of each cycle, the specimen was under tension only in 22 ms (~ 15% of the time) and during the reminder 120 ms the specimen is unloaded. The span and speed of this loading on the sling is roughly comparable to that induced by blinking the eye in vivo.

Therefore, considering the aforementioned parameters and as shown in Figure 17, in each cycle the maximum speed of the sling specimen upper end occurs at points **B** and **D** and is equal to

$$v_{max} = -2\pi\,(7\text{ Hz})\left(\frac{35}{2}\right)\sin(160.5^\circ + 180^\circ) = 256.8\text{ mm/s}$$

This value is in the range of the maximum voluntary eye blinking speed measured by Kwon et al. [79], i.e. around $250\ \mathrm{mm/s}$. We have chosen our parameters to induce this maximum speed in the sling specimens so that they undergo the same maximum speed during an eye blinking.

The specimen is under tension only from **B** to **D** for each **A-A** cycle as illustrated in Figure 17. The maximum strain in the specimen occurred at **C** and the maximum loading rate corresponds at **B** and **D**. In these experiments, the specimens are stretched to a specific displacement ($\delta = 2\mathrm{mm}$) in each cycle and are tested under the constant strain amplitude of $\epsilon = \frac{2\ \mathrm{mm}}{100\ \mathrm{mm}} = 2\%$. We believe that the constant strain fatigue test of the frontalis suspension slings simulates the physiological conditions in the body more realistically comparing to the previous studies done since in vivo conditions, the sling deforms in each blinking event for the same amount of displacement.

The error in the number of cycles to 0.25% accumulated permanent strain, i.e. the failure criteria in this study, was taken to be the maximum of two values: (1) the number of cycles between each two consecutive permanent strain measurements (resolution of the readouts) or, (2) the standard deviation of replicate experiment results.

This preliminary testing was temporarily interrupted at least every 8 hours to evaluate any progressive increase in plastic strain in the material under non-symmetric cyclic loading (also referred to as strain ratcheting). This permanent strain was evidenced by an increase in the minimum position at which the material specimen becomes completely straight (position y_s) as shown in Figure 18.

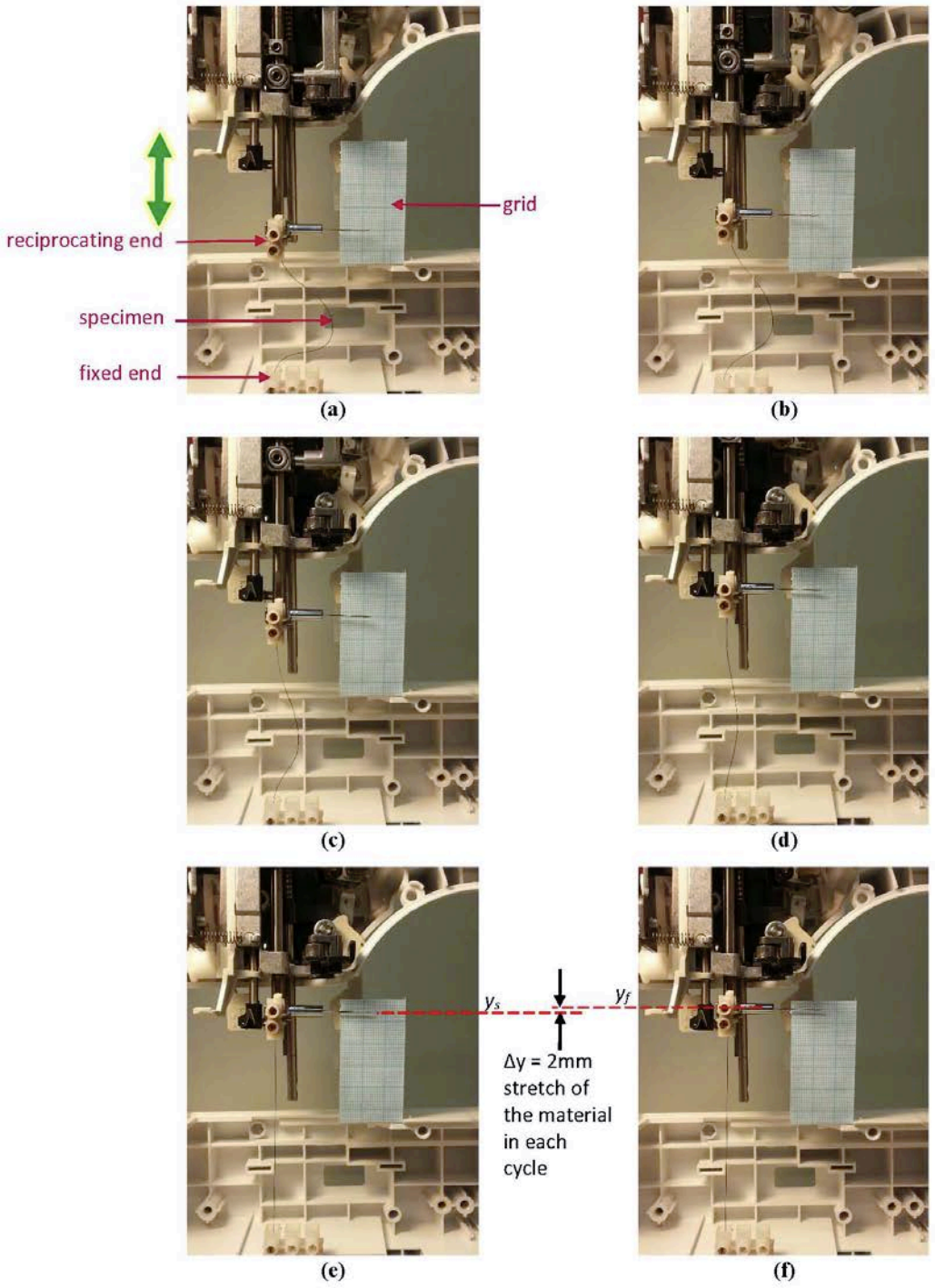

Figure 18: Photographs of the test system at six consecutive stages (stages a-f) of one loading cycle. The sling specimen is under stretch only during stage (e) to stage (f).

The material specimens were tested in two conditions: one in air at room temperature (25°C), and one while soaked in 0.9% saline solution and at 37°C (by setting the room temperature to 37°C) to simulate an interstitial environment and to avoid dehydration effects in the biologic materials. An illustration of the experimental setup with saline bath is shown in Figure 19.

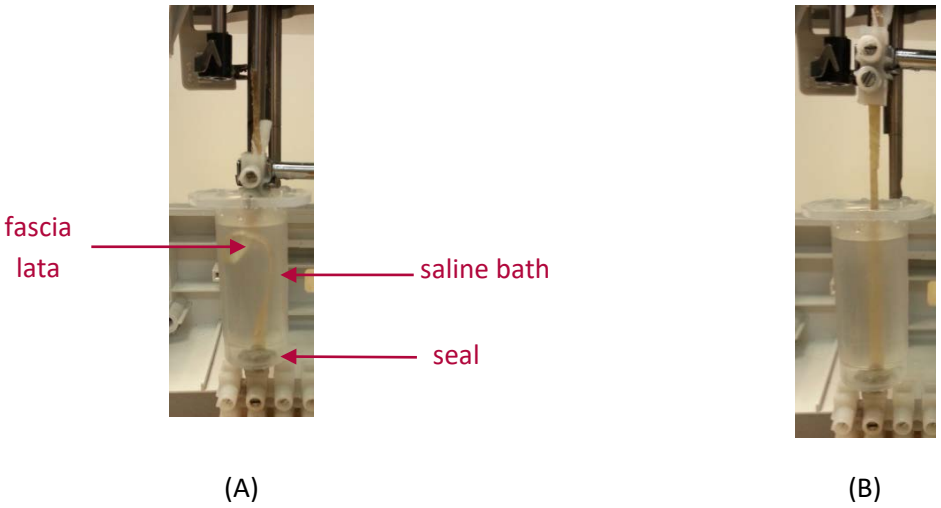

Figure 19: Implementation of saline bath into the setup. The sample in this figure is fascia lata when it is at (A) zero strain, and (B) at maximum imposed strain.

Three common sling materials were tested with our setup: 1) nylon monofilament 4-0 suture (Ethilon), 2) silicone elastomer (bvi Visitec frontalis suspension set), and 3) fascia lata. Each aforementioned sling specimen is a representative of the three material families that are used as frontalis suspension slings, i.e. thermoplastics, silicone elastomers, and tissues. Both fresh and processed fascia lata specimens were tested. The width of both fresh and processed fascia lata specimens were 0.3 cm, a standard dimension used in frontalis suspension [78]. Figure 20 shows each of three sling samples that were tested in the both considered conditions: 1) in Air, and 2) in saline.

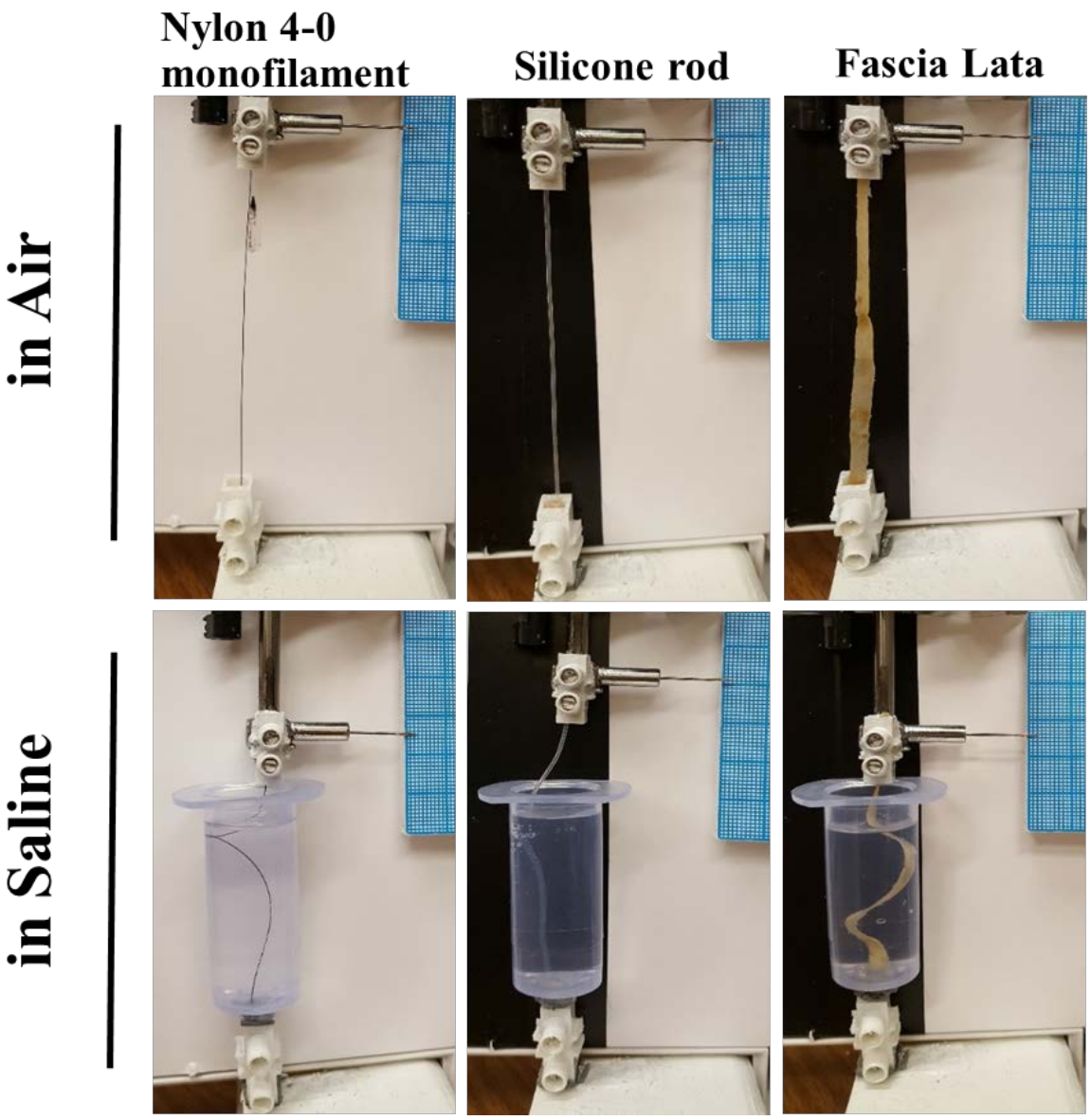

Figure 20: All the different sling specimens and the conditions that were tested.

All samples were stretched Δy = 2 mm during each cycle. Since the different sling materials tested here have different stiffnesses, the maximum load that is generated in each sling material was different. However, Δy = 2 mm maximum stretch was chosen such that the maximum load generated in the slings is in the range of the force applied by the eye muscles to the frontalis sling,

i.e. a load amplitude in the range of ~0.7 - ~2 N (see Table 9 for the measured mechanical properties of the sling specimens).

Table 9: Measured geometrical and mechanical properties of the sling specimens tested in this study

Sling type	**Geometry and cross section area (A) [mm^2]**	**Spring constant [N/m]**	**Maximum applied force [N]**	**Elastic Modulus [MPa]**	**Maximum applied stress [MPa]**
Nylon 4-0 monofilament	D=0.18 mm A= 0.025	627	1.80	616.8	57.0
Silicone	D=0.9 mm A= 0.636	157.5	0.67	1.06	1.06
Fascia Lata	W = 3 mm t = 0.41 mm A= 1.23	1015	2.10	20.6	1.71

A value of permanent elongation equal to 0.25 mm (0.25% plastic strain) was selected as a test endpoint since it corresponds to the minimum discernible and quantifiable amount of plastic elongation that can be measured in the preliminary setup. Considering that eyelid drooping and MRD (Marginal Reflex Distance) changes have been reported in some cases by 0.25 – 0.5 mm resolution [80], the present 0.25 mm plastic elongation criterion can possibly have clinical significance. The sling specimens were measured both before and after each experiment and examined using optical microscopy.

Each material under investigation was tested three times, i.e., with a new specimen in each experiment. The number of the total cycles that led to plastic elongation was averaged for each material. The number of loading cycles was calculated using the following equation,

$$N = f \times \Delta t$$

Where f is the frequency of cyclic loading, and Δt is the test duration. Cyclic loading speeds of 1.2, 7, and 15 Hz were confirmed for this setup using high-speed video recording that were analyzed using ImageJ software [81]. In order to minimize observational error, a magnifying glass was used to determine the permanent displacements of the specimens.

Results

Nylon monofilament 4-0, silicone rod, fresh fascia lata, and processed fascia lata specimens each exhibited physical changes under cyclic loading conditions. The test results are reported in Table 10.

Table 10: Fatigue test results for different sling materials tested in air and saline

Material	*Tested in Saline*	*Number of Cycles to 0.25% Plastic Strain*[†]	*Notes*
Nylon monofilament 4-0	No	N/A	No elongation occurred up to 15M cycles
Nylon monofilament 4-0	Yes	N/A	Decrease of diameter at ~5M (± 500K) cycles
Fresh Fascia Lata	No	~818 K (± 200K)	
Fresh Fascia Lata	Yes	~1.9 M (± 350K)	
Banked Fascia Lata	No	~750 K (± 200K)	
Banked Fascia Lata	Yes	~1.2 M (± 300K)	
Silicon	No	~184 K (± 25K)	
Silicon	Yes	~150 K (± 30K)	

* K: thousand
* M: million
[†] For definition of failure, refer to Materials and Methods.

No significant permanent elongation was observed for nylon 4-0 sutures up to 1.5×10^7 cycles. However, a decrease in the diameter in a central region of nylon suture occurred after approximately 5×10^6 ($\pm 5 \times 10^5$) cycles (Figure 21). Overall, the Nylon 4-0 suture specimens were found to be the most resistant material to strain ratcheting, with fresh fascia lata, processed fascia lata, and silicone exhibiting lower resistance respectively (Figure 22). Silicone exhibited permanent elongation very early compared to the other materials.

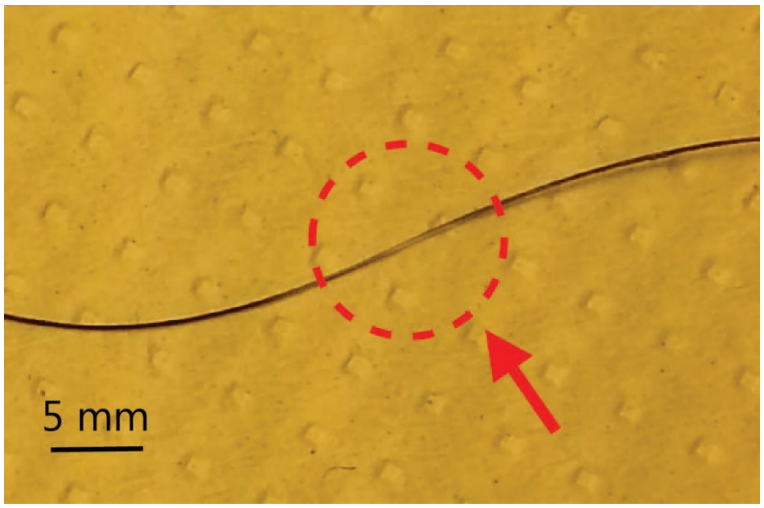

Figure 21: Optical micrograph showing a localized decrease of diameter in a 4-0 nylon suture tested to 1.5 x 10^7 cycles.

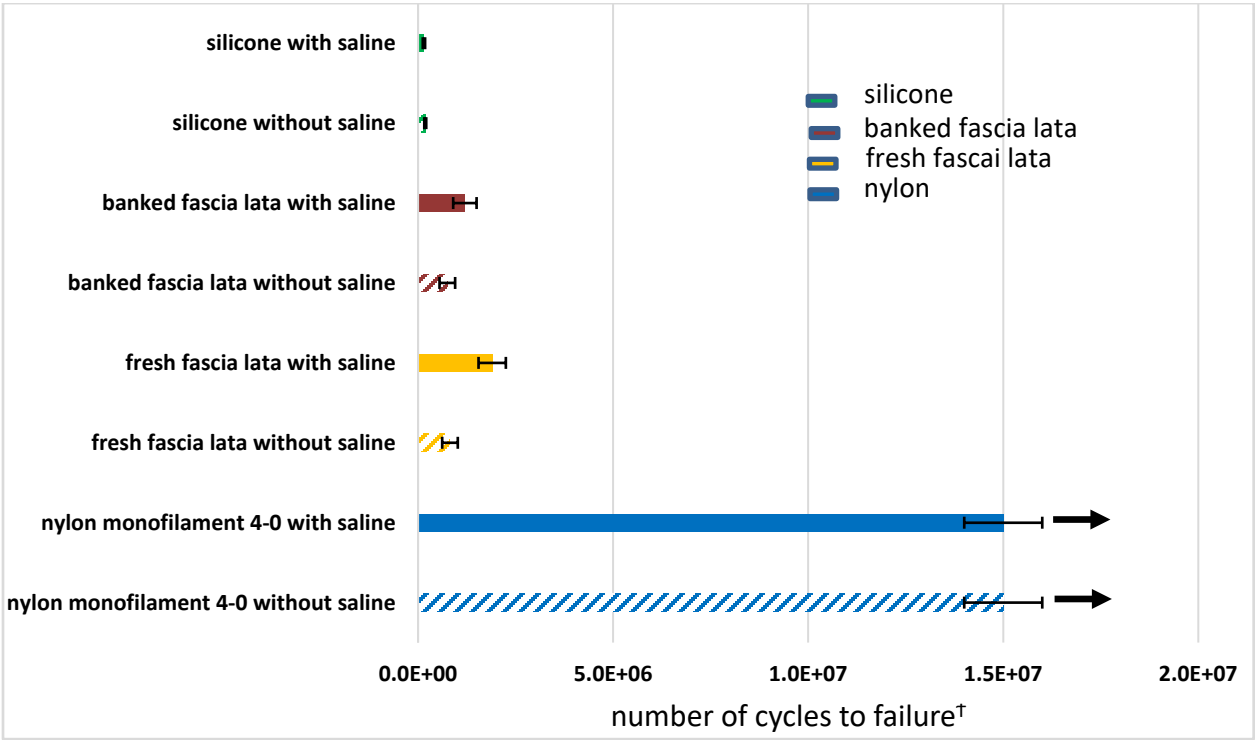

Figure 22: Graphical representation of results for different materials. The silicone specimens permanently elongated to 0.25% within 8 hours. The smaller error bars for silicone are due to more frequent monitoring compared to the other tests.

Discussion

Frontalis suspension blepharoptosis repair is performed with a wide variety of materials. There have been no prospective, randomized studies comparing eyelid suspension slings and consensus on the material with the best overall properties and profile is lacking [5], [41]. The present proof of concept study adds to the few studies formally evaluating the effects of physical strain on commonly used suspension materials [40], [60], [61] as described in the following.

The present preliminary study showed a wide variability among different eyelid suspension materials subjected to identical cyclic strains. Cyclic loading induced plastic (permanent) elongation to silicone, and fascia lata strips. Nylon 4-0 seemed to be the most resistant to plastic elongation by cyclic strain ratcheting. An unexpected finding was the thinning of the central region of nylon sutures during cyclic loading. This thinning and formation of a ribbon shape morphology in nylon under cyclic loading could be due to a *crazing* mechanism under the imposed fatigue conditions. Crazing under cycling loading takes place in many polymers, because the material is held together by a combination of weaker Van der Waals forces and stronger covalent bonds. Adequate local stress vanquishes the Van der Waals forces, permitting a narrow gap to form between polymer chains. These gaps, crazes, form at highly stressed regions associated with scratches, flaws, stress concentrations and molecular inhomogeneities. Crazes can be seen because light reflects off the surfaces of the gaps. The white color observed in the present thinned region of nylon specimen could be caused by light-scattering from the crazes. [82]–[84] . The importance of segmental thinning of the nylon in vivo is uncertain, but it can be hypothesized that it may be associated with the rearrangement of polymer chains during crazing and a loss of toughness and

increased risk of fracture. Additionally, thinning may pose a greater risk of "cheese wiring" or cutting through soft tissues [5]. Further investigation should be performed to clarify these risks.

Silicone was particularly prone to relatively early permanent elongation compared to the other materials tested in the present preliminary study. The clinical significance of its observed early ratcheting is uncertain. However, it can be surmised that this elongation may be associated with a greater incidence of undercorrection, ptosis recurrence, or both, compared to other slings. Silicone requires a slightly greater tightening than fascia to achieve the same amount of lid margin lift, with all other variables and techniques equal. However, early permanent elongation of silicone must be balanced against other favorable features of silicone such as low bioreactivity, availability, no morbidity of a second surgical site, and ease of handling.

An additional notable finding was the differences between fresh and processed fascia lata. Irradiation or lyophilization in processed fascia [41], [68] may disrupt internal chemical bonds to explain earlier development of permanent elongation compared to that for fresh fascia. Dehydration and rehydration of processed materials may also contribute to reduction in yield strength [69].

Further studies comparing mechanical property changes of biological grafts due to processing may be insightful. Prior studies have evaluated the clinical endpoint of surgical success with various suspension materials in vivo [5], [41]. Interestingly, these data corroborate those findings with the exception of the nylon suture that has repeatedly been found to have a high in vivo rate of failure [48]. As mentioned above, other factors may be contributing in these cases.

Limitations of the present preliminary study include the in vitro test system. Degradation of the nonpreserved biological slings may be a confounding factor. Although our experiments attempted to simulate an in-vivo environment in temperature and tonicity, the amount of physical force applied to the slings may be inaccurate. The stretch-relaxation cycle and amount of force may vary with the amount of strain on slings implanted in the eyelid, i.e., in vivo. In addition, the present experiments were terminated at 1.5×10^7 cycles. As stated previously, an implanted sling may undergo significantly greater cycles.

A further limitation of the present study is the narrow selection of implants. A wide variety of materials can be used in these sling procedures and include fresh (autogenous) or processed (banked) fascia lata and alloplastic materials that include chromic gut, collagen, polypropylene, silicone, stainless steel, silk, supramid, nylon monofilament, polyester, and polytetrafluoroethylene (PTFE) [5]. In addition to other materials, different dimensions of the same material may yield dissimilar results [85].

In summary, the experimental data provided in this chapter offer a proof of concept that permanent structural changes occur in frontalis sling slings with cyclic loading. Further investigation will clarify the clinical relevance, but these initial findings may contribute to our understanding of frontalis suspension and other grafted sling-type procedures where the implanted devices undergo significant cyclic stress.

Chapter 4

Development of a New Fatigue Test System to Study Sling Materials under Physiologically Relevant Conditions

In the next phase of our studies on the sling materials we decided to improvise another setup for testing the sling materials that address the limitations of previous setup. The limitations of the previous setup (discussed in Chapter 3) are as below:

1- There was no way to measure the instantaneous tension in the slings. In the previous setup, the only way to estimate the load was to correlate the amount of strain to the stress in the material assuming its elastic behavior is linear and known.

2- In order to measure the permanent elongation, the test needed to be interrupted. This interruption could introduce some level of recovery and relaxation to the specimen and therefore interfering with the final results. Moreover, since the occurrence of plastic elongation and its amount was identified by distinguishing the position at which the specimen transitions just from the slacking condition to the straight condition visually, this distinguishing could be subjective in some cases and influence the results.

3- The saline bath design was such that the sling was not always soaked in the saline solution and the bath needed to get refilled more frequently due to occurrence of saline splashes outside of the bath as the upper grip went inside and outside of the bath frequently during the test.

4- The temperature of the saline solution was not controlled and only the temperature of the room in which the setup was held was controlled, which could easily change due to opening and closing the room door or changes in the room air conditioning system.

5- Due to the design of the setup, the sling was not always under stretch and was slacking in most part of the cycle. It might be more physiologically relevant to have the sling always under some level of tension.

6- Due to the limitations in the size and design of the setup, there were limitations on how much stretch could be applied to the sling in each cycle.

7- The frequency of the loading was not adjustable and the studies could be just done in three different frequencies of 1.17 Hz, 7 Hz, or 15 Hz. However, all the tests have been done in the 7Hz mode because the other two frequencies were either too slow or too fast for the tests. Furthermore, the machine was not stable enough at 15 Hz.

8- Since the two ends of the sling were just gripped by compression via grips, there was a large stress concentration at the two sling ends. This could result in increased probability in rupture of the sling at the two ends and therefore voiding the tests.

Moreover, there was a high chance of slipping of the specimen from the grips or breaking of the sample at the grip faces. In some cases, the grips were not able to grip the specimen firmly due to the grips non-standard shapes or dimensions.

Addressing the *Preliminary Setup* limitations by developing a *New Setup*

Due to all the aforementioned limitations with our proof-of-the-concept setup, it was decided to develop another setup that addresses these shortcomings. We acquired a new fatigue testing machine (Fatigue Dynamics, Model DS-2000, Dearborn, MI) and adjusted, redesigned, and modified and this machine to the application considered in this dissertation, i.e. fatigue study of eyelid slings under physiologically relevant conditions. For developing this new setup, we took all the limitation with the proof-of-concept setup that were discussed before into consideration. The new setup was developed such that it addresses all those limitations.

Some of the advantages of the new developed setup (see Figure 23) to the older setup (proof-of-concept or preliminary setup as discussed in Chapter 3) are as below and listed in the same order as the aforementioned limitations:

1- In order to monitor the force in the sling during all cycles, a load cell was integrated to the setup. The details about the chosen load cell are discussed later in this chapter.

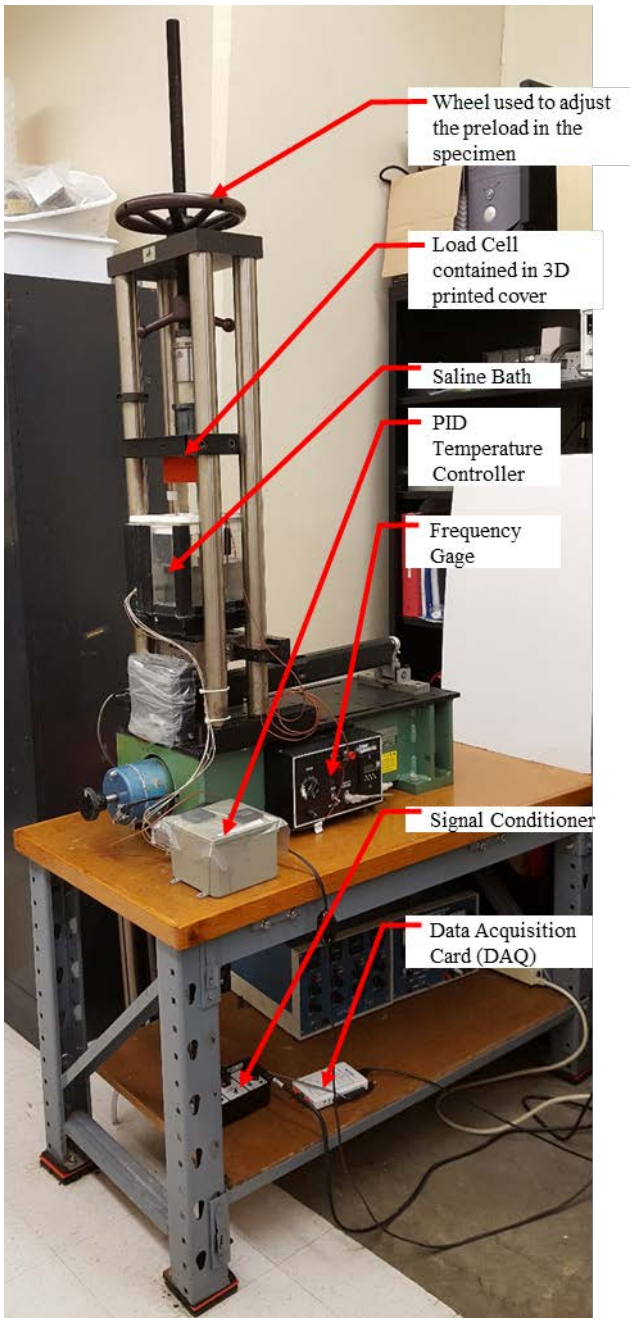

Figure 23: New developed setup for the fatigue behavior study of different slings under physiologically relevant conditions. Main features of the setup are labeled in this figure.

2- A laser scanning system was adapted to this setup. When needed, this system could be integrated to the setup to allow non-contacting, unattended monitoring of the strain in the

sling sample during each cycle. Figure 24 illustrates the whole setup when the laser scanning system is also integrated.

Figure 24: Laser Scanning System integrated to the setup to monitor the induced strain in the sling during the fatigue tests

3- A larger saline bath with the dimension of 7”× 7”× 7” was included is this setup. The saline bath was made out of transparent plexiglass to allow visual checking of the specimen during the test.

4- The temperature of the saline solution was controlled to be at the physiologically relevant 37°C, which is the normal human body temperature. A PID control system was used to maintain the temperature of the saline solution inside the saline bath at 37°C.

5- In this setup we could adjust the specimen to be always under tension during the test. The amount of preload in the sample could be adjusted by means of a handwheel on top of the load tower in the setup as shown in Figure 23. The tension in the sling sample oscillated between a minimum and maximum number during each cycle. Having the sling sample always under tension during the whole cycle is more physiologically relevant than what we had in the preliminary setup.

6- In this setup, the amount of stretching in each cycle was adjustable through setting the amplitude of stretching during each cycle via a crank-shaft mechanism as illustrated in Figure 25.

Figure 25: The crank-shaft mechanism included in the rear of the setup is used to adjust the amplitude of stretching in each cycle.

7- In this setup, the frequency of the sinusoidal cyclic loading was adjustable from 3 to 40Hz. Although we were able to perform some tests on the slings under loading frequencies as low as 0.5Hz, the loading was not completely sinusoidal during cycles with frequencies less than 3Hz (see Figure 26); the effect of gravity on increasing the angular inertia in the crank during its rotation from its highest position to its lowest position was the reason for not getting a uniform complete sinusoidal loading scheme in frequencies less than 3Hz. As the frequency of loading goes beyond 3Hz, the angular inertia generated by the motor could overcome the effect of the gravity.

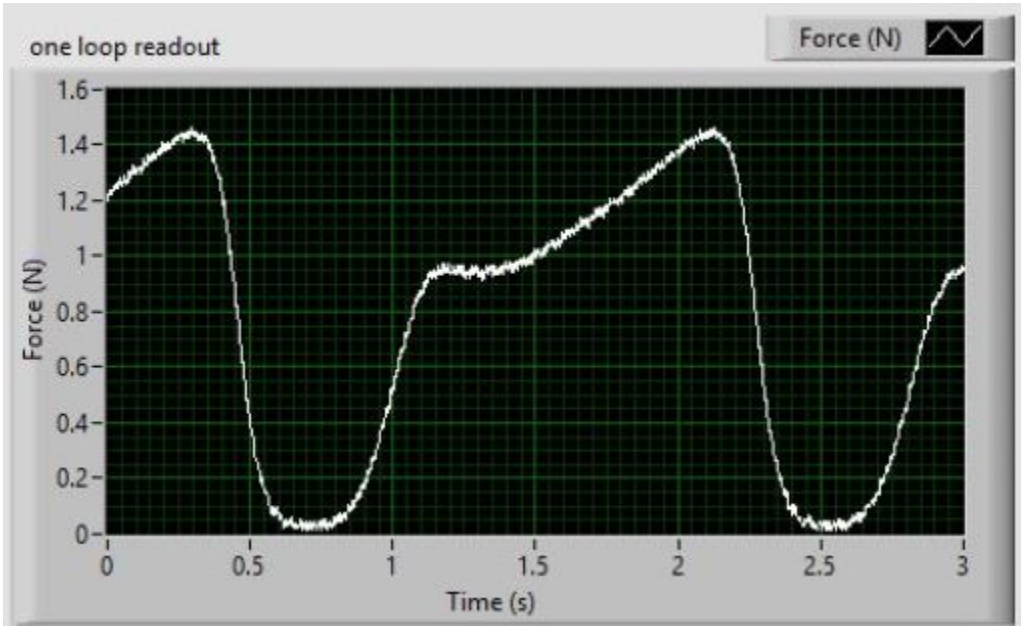

Figure 26: An example of the provided non-sinusoidal loading cycle when the set loading frequency is less than 3 Hz. In this case the loading frequency is around 0.5 Hz.

In this setup, in order to prevent the breakage of the specimen in the clamping area and minimize the local stress concentration in the sample at where it leaves the grips, new grip designs have been implemented and tested. Grip-induced failure through stress concentration was obviated with the use of specially constructed clamps in which the sling is wound around non-rotating cylinders after

getting secured by clamps as illustrated schematically in Figure 5. These grip designs were based on the test standard specifications and guidelines from ASTM. Specifically, the non-rotating cylinder design and specification were based on ASTM D5034-09(2013) test standard [86]. Another ASTM test protocol that was considered partially for designing the system include: ASTM E-606/E606M-12 [87]. More details about the different tried grip designs for this work will be discussed later in this chapter.

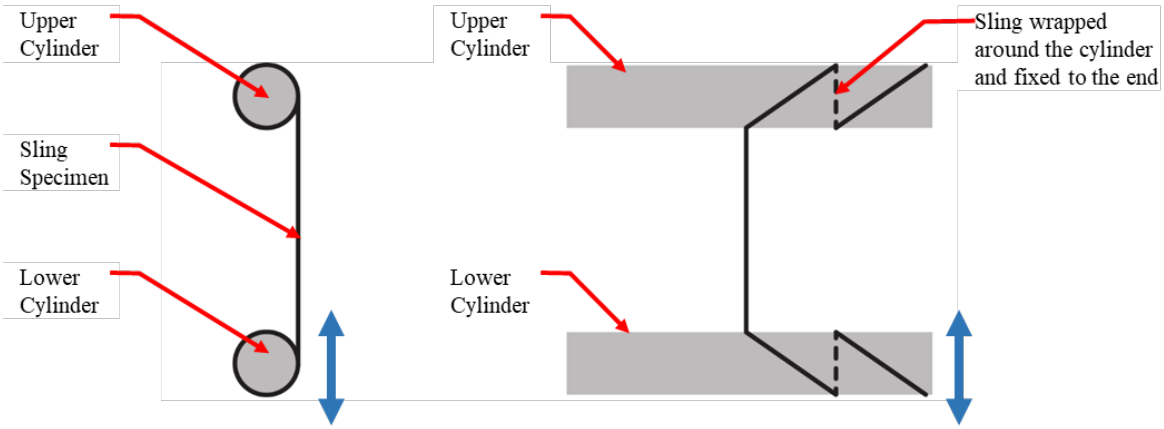

Figure 27: Side view and front view of how the sling specimen is wound and fixed around the non-rotating cylinders to obviate the stress concentration. In this setup the lower grip provides a reciprocating movement. When the specimen is under enough preload, it will always be stretched during the cycle.

The new sling fatigue testing system details

Different sling grip and clamp mechanism designs

In the first tried out design for gripper that is consistent with the aforementioned standards, we decided to have the sling get clamped on the same cylinder that it is wound around. This idea (Version 1.0 design) is illustrated in Figure 27. As shown in this figure, the lower end of the sling is gripped to the lower cylindrical grip which is oscillating with the desired frequency and

amplitude. The Upper cylindrical gripper is fixed but its height can be changed to induce different preload in the sling. To safeguard axial tensile stress within the gage length, the axis of the test specimen should coincide with the center line of the heads of the machine. The different methods for clamping was tried with this idea. The first method was to use an outer flexible hollow cylinder to fix the sling buy pressing it to the cylinder (as shown in Figure 28 for testing fascia lata in saline solution).

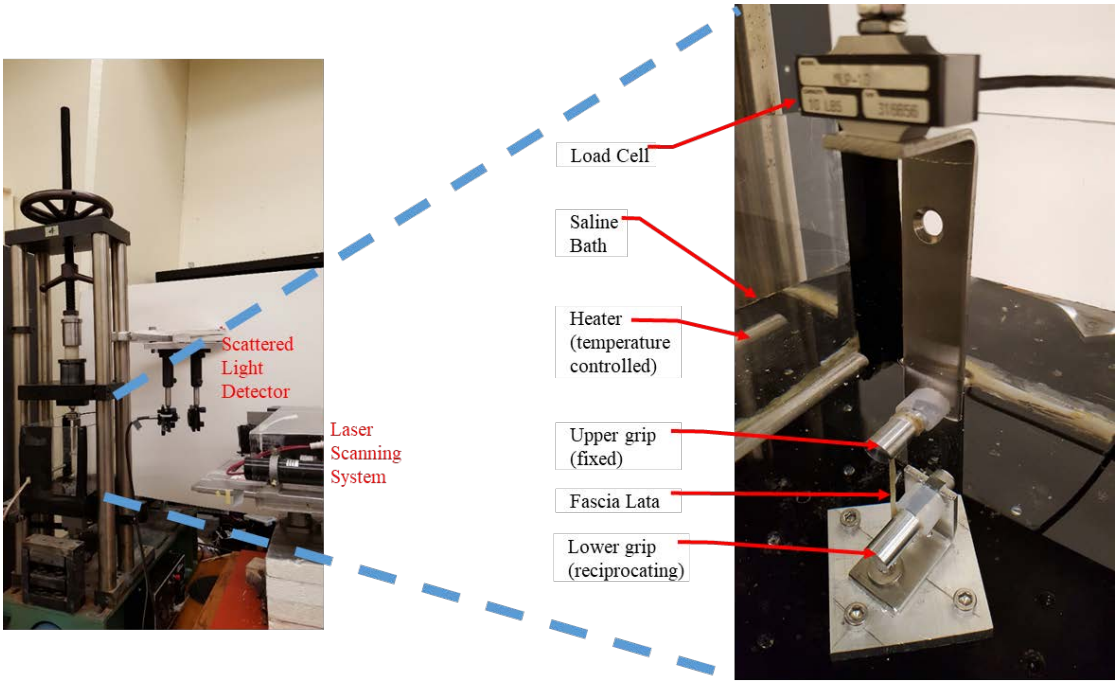

Figure 28: The whole experimental setup and the saline bath: This figure depicts how the cylinder grips are located in the in the whole designed experimental setup (Version 1.0 design). The specimen in this case is fascia lata tested in saline solution. The clamp for cylinder grips is made of a white Polyethylene flexible hollow cylinder.

The second method was to clamp the sling specimen between an inner cylinder and an outer hollow shaft that has an inner diameter slightly larger than the diameter of the shaft. The hollow shaft is screwed to the inner cylinder. The third method was to have the inner shaft (cylinder) and outer hollow shaft eccentric. One screw pushes the inner shaft to the inner surface of the hollow shaft

and grips that sling end on the opposite side. After the sling is gripped, it is wound one or more times around the cylinder and leaves the cylinder (see Figure 29 for the schematic of this design and an experiment example done for silicone sling specimen in saline solution with this design). It then winds around the other shaft and gets gripped by the other hollow shaft to that cylinder. The advantage of this gripping method compared to the other ones was that just one screw was enough to fix the position of the sample. The disadvantage was that it sometime is difficult to have the sling end get fixed on the side of the shaft opposite to the screw.

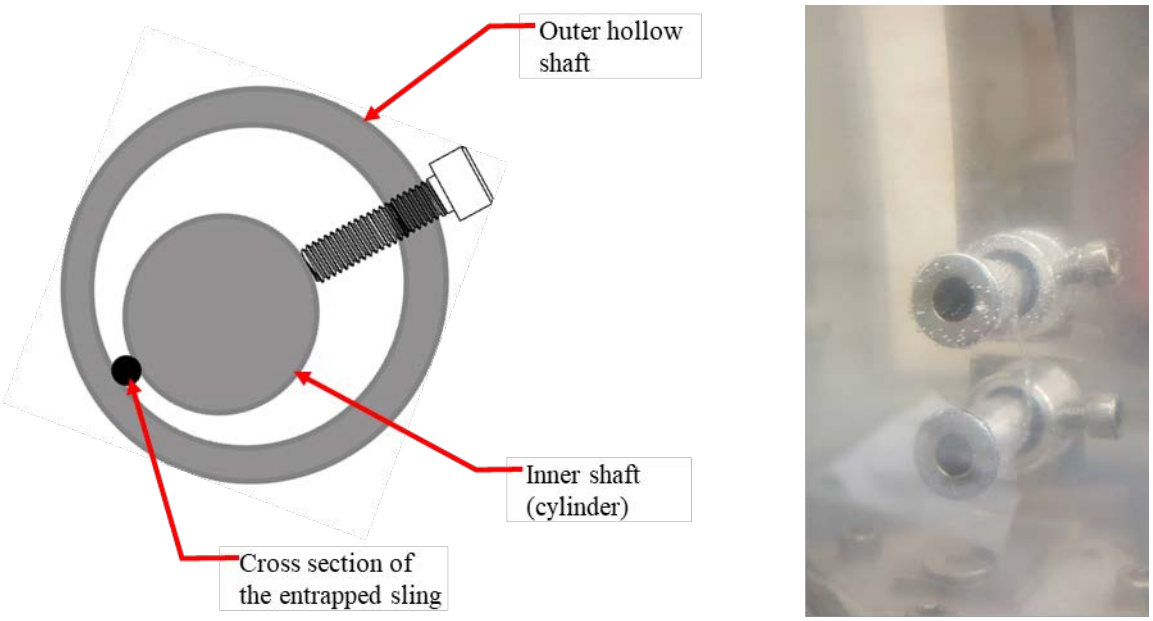

Figure 29: schematic and real picture of how the sling specimen (silicone in this case) is clamped in Version 1.0 of the setup before winding between the inner cylinder and an outer hollow shaft

All the aforementioned inner cylinder and outer clamp were machined out of aluminum. After performing multiple fatigue tests in 37°C saline solution, it was noticed that pitting occurs in all the aluminum parts. Therefore it was decided to manufacture all the next generation on the gripping mechanisms out of stainless steel instead of aluminum.

The upper grip is attached to a load cell. The load cell outside of saline solution and is stationary. The fact that the load cell does not oscillate prevents additional occurred noises in the read out of load cell. In order to prevent splashes of saline solution to the load cell, a 3D printed cover was designed and built for the load cell to cover it and save it from possible splashes of saline during the test. Moreover, a Styrofoam lid was used to prevent splashes of saline solution outside of the bath. This lid also helps prevent the water evaporation and maintain the saline temperature.

In order to overcome the complications of the first method of clamping the sling specimen to cylinder, it was decided to clamp the end of the sling not on the cylinder, but to the arm that holds the cylinder (see Figure 30 for Version 2.0 of the setup). Three different clamping methods have been used here. The first method was to use a simple plastic clamp with flat ends. The second method was to use stainless steel clamps. And the last and the best method was to clamp the sample end to the arm by just one stainless steel plate (tab) that is fixed to the arm by just one screw. The sample end gets fixed between the arm and the tap by just rotating the screw as shown in Figure 30.

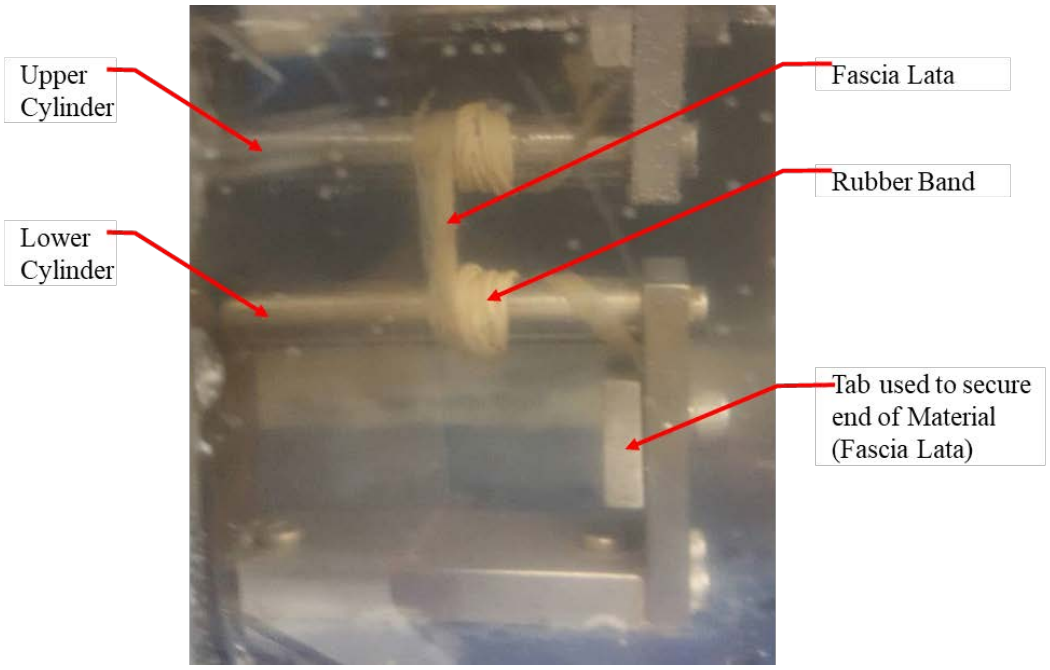

Figure 30: Fascia lata sample under fatigue test in Version 2.0 of the experimental setup. Note the change in the design of the upper and lower cylinder grips and clamps (tap clamp in this case). Every part of the setup soaked in saline is made out of 316 stainless steel in Version 2.0

One important point that should be noticed is that when the upper stainless steel arm is attached to the load cell, there should be complete electrical insulation between the screw and the load cell, otherwise, this could be a source for noise and ground loop in the whole system circuit.

It should be noted that 37°C saline environment is a very corrosive environment. During the course of our test, several parts of our setup failed because the splashed saline solution remnants speed up the corrosion fatigue rate in the system part. Even springs in the setup that are out of the saline bath failed because of splashes of saline gradually led to growth of cracks and hence failure. It is suggested to cover all springs to prevent corrosion fatigue of these parts.

Laser Scanning System details

This system scans a laser beam over a vertical line that overlaps with the specimen. This high speed laser scanner that was already developed at UCI [88], [89] was used to measure the spacing between two reflective marks, silver paint spots, or reflective tape strips on the sample. The measured spacing can provide us with the information about strain and possible plastic elongation in the sample.

Developing the software for the new setup

The software for the setup was developed in the National Instruments LabVIEW environment. Several Virtual Instruments were developed for calibration, data acquisition and analysis. To calibrate the load cell and convert voltage readings into Newtons, weights ranging from 10-200 grams were hung from the load cell to create several data points which were used to draw a linear trendline. The trendline was added within the code to convert the voltage readouts to Newtons. This calibration was performed before every test.

To collect force data, the load cell (MLP-10 or MLP-50 Transducer Techniques) would transmit data to a data acquisition card (National Instruments MyDAQ). The output signal from the DAQ is later amplified and conditioned via a Signal Conditioner (Transducer Techniques TMO-2) which then passed the data to custom LabVIEW Software in real-time. The sampling rate was 1000. The developed Virtual Instrument (VI) shows the present loading cycle in real time. It also finds the minimum and maximum load in each cycle and at specific interval and plots them. Therefore, the VI can provide the maximum and minimum sling load history. Figure 31 illustrates the front panel

of the main VI for load cell data collection and analysis. This VI provides the sling load changes data under the fatigue conditions.

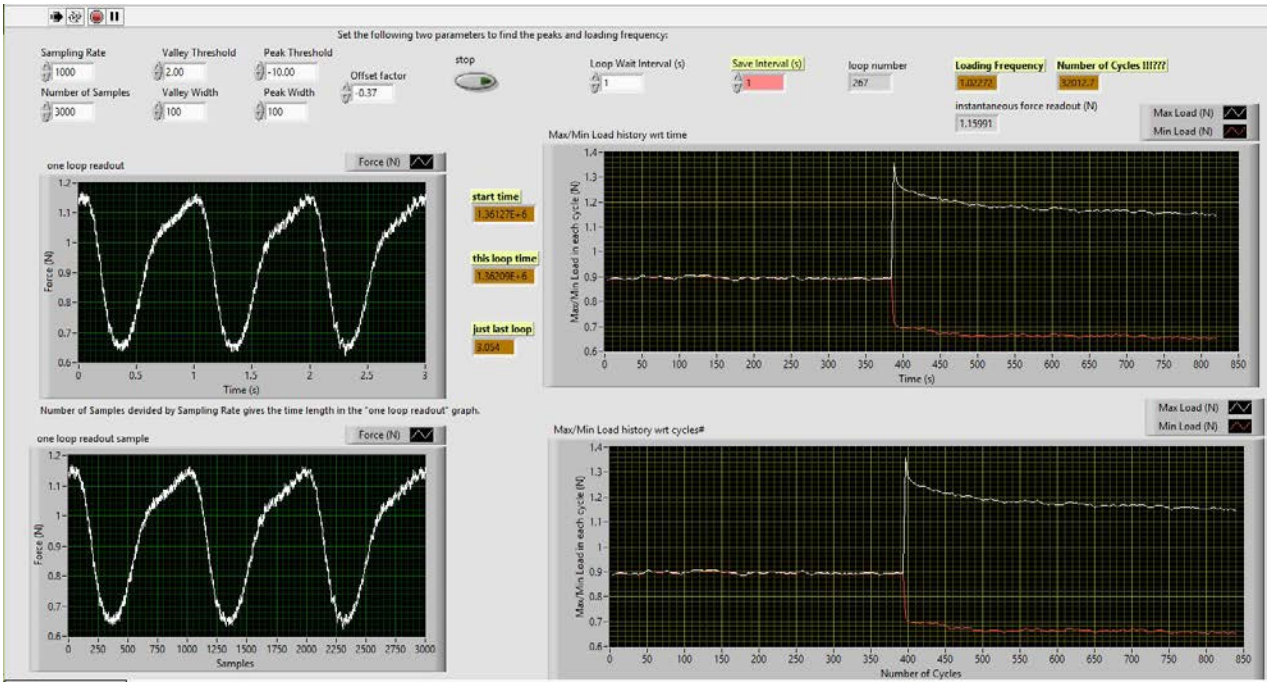

Figure 31: Font panel (user interface) of the developed main LabVIEW VI for data collection and analyses from the load cell. Left side graphs show the load cell readout and right side graphs show the history of the maximum (white curve) and minimum (red curve) applied forces throughout the test.

Having the sling sample always under tension during the whole cycle is more physiologically relevant than what we had in the proof-of-concept setup. However, it is noteworthy that in some cases depending on the sling material and amount of minimum stress in the sling sample, the minimum stress could reach zero after several cycles and therefore a slack occurs in the sample leading to not having the sling always under tension in the subsequent loading cycles of the test. In conclusion, the more sophisticated developed experimental setup discussed in this chapter addresses the limitations of the preliminary experimental setup discussed in Chapter 3. To our

knowledge, this is the only experimental setup developed specifically to investigate the fatigue behavior of frontalis suspension sling materials under the physiologically relevant conditions. Nevertheless, the application of this experimental setup cannot be limited to in-vitro investigation of frontalis suspension slings. It can easily provide the capability to investigate the implants that are used in applications other than frontalis suspension procedure.

Chapter 5

Results of the Experiments with New Fatigue Test Setup

Many experiments were performed during and after the course of development of a "New Fatigue Test Setup" for studying of the sling materials. In the present chapter, the results for the most reliable and relevant to sling tests experiments are provided. Discussion, modeling, and interpretation of the results are also included. Several sling materials as well as other materials were tested on the present setup. Specifically, results for Nylon monofilament 4-0 suture (Ethilon), Silicone rod (bvi Visitec), and banked fascia lata (4mm wide strip) are presented and discussed. Further tests were performed on stainless steel spring wire, PTFE, Prolene, and Vicryl sutures during the course of setup development; their results are not included in this dissertation but are recorded separately.

Experiment parameters selection

The parameters for all these experiments were set to mimic the loading conditions that slings experience under physiological conditions during eye blinking. In one study, Senders et al. reported the force requirement to create an eyelid blink with an eyelid sling implanted alongside

and parallel to eyelid margins of a cadaver to be somewhere in the range of ~0.5N to ~1.7N [90]. Moreover, in another study from 1957, the orbicularis oculi muscle strength has been reported as 60-70 g (i.e. 0.6-0.7 N) in healthy subjects [91]. Other non-published studies have reported preliminary results of 0.2N and 1.8N required force for respectively normal and forced eyelid closure. Therefore, we assumed for our studies that the required force for opening and closing of the eye should be some number in the range of 1N to 2N.

It was decided to perform the fatigue tests under strain control since during eye blinking, the eyelid margin displaces for a constant amount and therefore it can be assumed that the inferior end of the sling that is attached to the tarsus plate moves for a constant amount equal to eyelid fissure (i.e. around 8 mm). Regarding the strain rate, different rates could be considered. One way is to mimic the actual eye blinking rate (around one blink every 5 seconds i.e 0.2 Hz blinking frequency). Another approach could be to run the tests such that the maximum speed of the sling specimen during each cycle is the same as the peak speed during each eye blinking, i.e. around 250 mm/s. The peak speed during blinking has been reported in several studies before. We have considered the most recent study on this issue which reports the peak blinking speed as 243±9 mm/s ≅ 250 mm/s [79]. We considered this criteria specifically before for the sling fatigue tests done with the proof-of-concept setup (discussed in Chapter 3).

The sling specimen moving end in the "New Fatigue Test Setup" oscillates in a sinusoidal manner with respect to time given as,

$$y = a\cos(2\pi f t)$$

where a is the maximum amount of stretch in each cycle and f is the loading frequency. Therefore, the peak speed of sling end during each cycle will be $v_{max} = 2\pi f a$. Hence having $fa = \frac{250\ mm/s}{2\pi}$

$\cong$ 40 mm/s takes reaching the same peak speed during blinking criteria into consideration. Considering our setup limitations, two applicable f and a parameter selection examples could be choosing ($f = 5\ Hz, a = 8mm$) or ($f = 10\ Hz, a = 4mm$).

The third consideration for choosing the frequency of the tests is selecting a frequency that is fast enough to perform the fatigue tests in a reasonable time frame. The test results that we are reporting here are performed by setting $a\ (the\ maximum\ sling\ end\ displacement) = 4mm$.

The amount of pre-stretch in the sling specimens were chosen such that the force applied by them before the start of the cyclic loading tests is in the range reported for the force generated by orbicularis oculi muscle, i.e. in the range of 1N to 3N. The length of the suture and loading frequency were set to cause a strain rate corresponding to that exerted by the blinking of the eye. The sample gauge length (length of sample) at F_{min} position was chosen to be 25 mm, i.e. the distance between the top of the brow and eyelid margin where the sling end is fixed to the tarsus plate.

Generally speaking, the test parameters were set for each material to mimic the fatigue that an implanted sling of that material would undergo. Because different sling materials have different elasticities, the same F_{min}–the minimum load in the sling in each cycle–among all slings could not be reached while the condition of having the same constant strain in all materials is also satisfied. Therefore, it was attempted to reach F_{min} values in all samples that are all in the same range by adjusting the prestretch (preload). However, the preload should be set such that the number of cycles to failure for the sample is not significantly affected.

Test Protocol

Regarding the results that are provided below, the following tests were done for each specimen in order: stress relaxation, 1 Hz fatigue test, stress recovery, 5 Hz fatigue test, stress recovery, and 10 Hz fatigue test.

For stress relaxation test, first each sample was securely mounted. The saline bath was filled with 0.09% saline solution and warmed up to 37°C and maintained at this temperature. It is very important to wait for the whole system to stabilize before starting the tests. In our setup, we suggest waiting at least 6 hours before starting the test so the whole setup temperature reaches steady state. While the system reaches steady state after adding the saline and warming it up to 37°C, a rise of around 0.2N in the load cell readout happens and therefore, if we do not wait for the system to stabilize, this error adds up and intervenes with the results.

After the system reaches steady state, the upper grip is raised up to elongate the sample to reach the desired prestretch (preload). Then the sample was held at this displacement and the load changes were recorded. As the time goes on, the sample relaxes and the load drops. In the stress relaxation test, we waited until the load in the sample reaches a steady state.

After the relaxation test, we started the fatigue test. To do so, the machine was turned on and the loading frequency is reached to the desired loading frequency quickly but gradually to minimize the sudden unexpected forces applied to the sample. Following each fatigue test, the cyclic loading of the samples were stopped and the sample was held at the F_{min} position. Depending on the material type and amount of the load in the material, the load recovers partially.

Experiment Results

Results for monofilament nylon 4-0 suture, silicon rod, and banked fascia lata are presented below.

Monofilament nylon 4-0 suture relaxation, fatigue, and recovery test results

After the nylon 4-0 monofilament suture sling specimen was mounted securely to the grips, the heated bath was filled by saline solution. Testing did not begin until the temperature of the solution reached 37°C and the load cell read-out stabilized. Afterwards, the upper grip was pulled to induce a 2.2 N force in the sling specimen. The specimen was then left in tension for an extended period of time and load changes dictated by relaxation of the specimen were recorded. Figure 32 shows stress relaxation results for a nylon 4-0 monofilament suture sling specimen. The tension inside the sling dropped to 1.55N (~30% reduction in the load) in a matter of around 135 minutes (2.25 hours). The relaxation test can model two cases regarding the sling behavior: one is the behavior just after its implantation in the body and before when the patient starts to blink, and a second is the behavior of the implanted sling when it goes under extended periods of constant tension for example due to eye closure when the patient is asleep. Stress relaxation during such periods may cause the nylon suture to no longer provide the sufficient force needed to elevate the upper eyelid at the correct position.

We were able to model the behavior of different sling materials under stress relaxation with two Maxwell dashpot-spring branches in parallel. Each Maxwell branch is composed of one spring with spring constant *k* and one dashpot with viscosity constant *c*. Using a curve fitting algorithm, the appropriate parameters for each Maxwell branch constant were determined from the experimental data. The parameter ε_0 is the constant strain applied to the sling specimen. The

diagram of the Maxwell branches and the magnitude of the constants are provided bellow each figure.

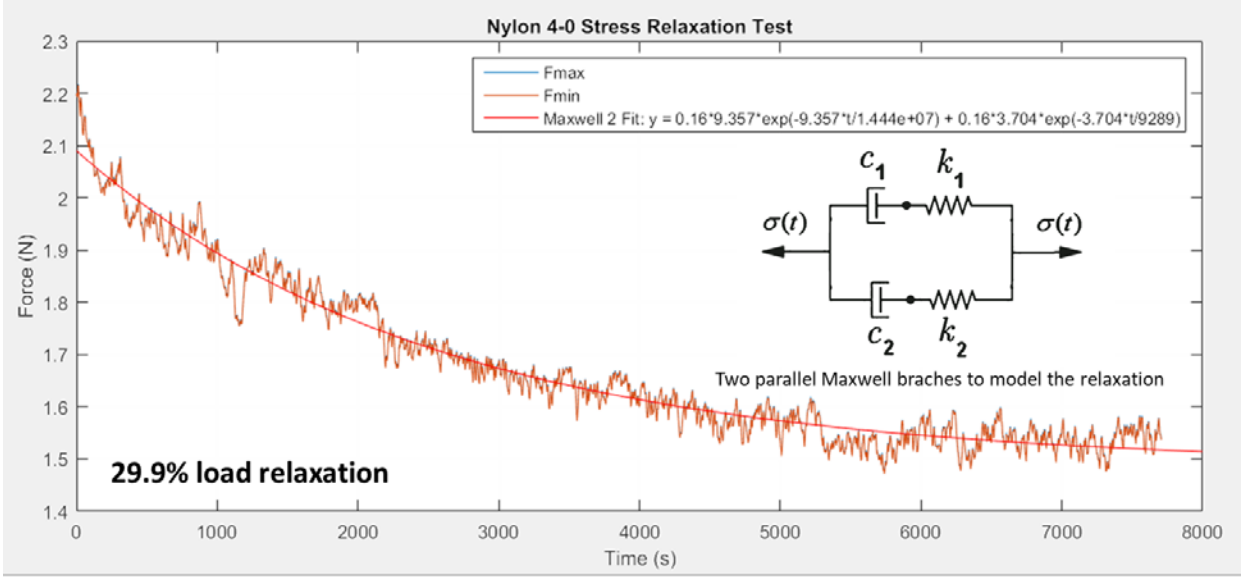

Sling type	Geometry and cross section area (A) $[mm^2]$	Spring constant $[N/m]$	Maximum applied force $[N]$	Elastic Modulus $[MPa]$	Maximum applied stress $[MPa]$
Nylon 4-0	D=0.18 mm A= 0.025	627	2.90	616.8	114.0

Nylon Stress Relaxation Test	
Coefficient	Value
ε_0	0.16
K_1	9.357
C_1	1.444e+07
K_2	3.704
C_2	9289

Figure 32: Stress relaxation in nylon 4-0 monofilament suture sling

Although we performed fatigue test of nylon monofilament suture at different loading frequencies and R-ratios (R-ratio = min strain or stress during the loading cycle divided by max strain or stress during the loading cycle), here we just report the result of fatigue test in 1 Hz mode and R-ratio = 0.4 N/ 2.9 N = 0.14 (see Figure 33). Interestingly, F_{max} dropped from ~2.9 N to ~2.5 N just in the first 10 cycles. After this sharp drop in stress in the first few cycles, F_{max} gradually dropped to ~1.9 N exponentially and stabilized during ~ 4×10^4 cycles. We were able to show that modeling with two parallel Maxwell branches can also describe the behavior of sling specimens under fatigue conditions. The relevant constants of Maxwell branches are also provided bellow each figure.

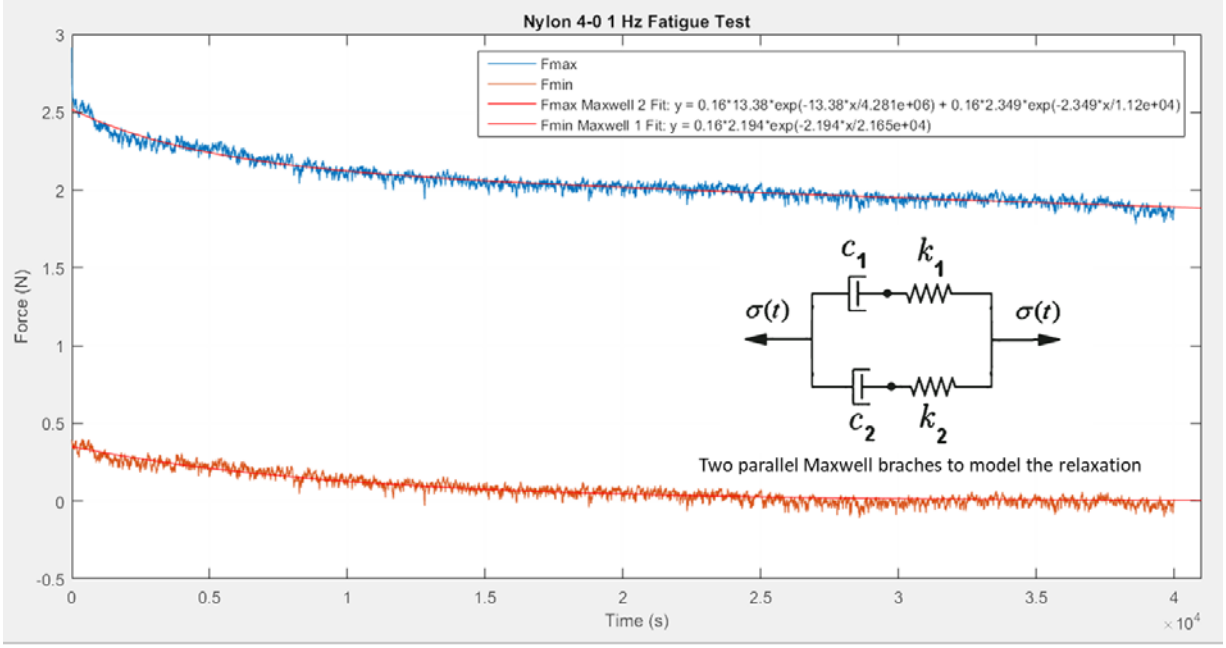

Nylon F_{max} 1 Hz Fatigue Test	
Coefficient	Value
ε_0	0.16
K_1	13.38
C_1	4.281e+06
K_2	2.349
C_2	1.12e+04

Nylon F_{min} 1 Hz Fatigue Test	
Coefficient	Value
ε_0	0.16
K_1	2.194
C_1	2.165e+04

Figure 33: Fatigue test result for a nylon monofilament 4-0 suture sling specimen at 1 Hz

Immediately following a fatigue test, we allowed the nylon monofilament specimen to sit at its position of minimum strain (F_{min} position) to determine whether or not there was any recovery in the load. During the recovery period, the load in the nylon monofilament sling increased for about 0.2 N.

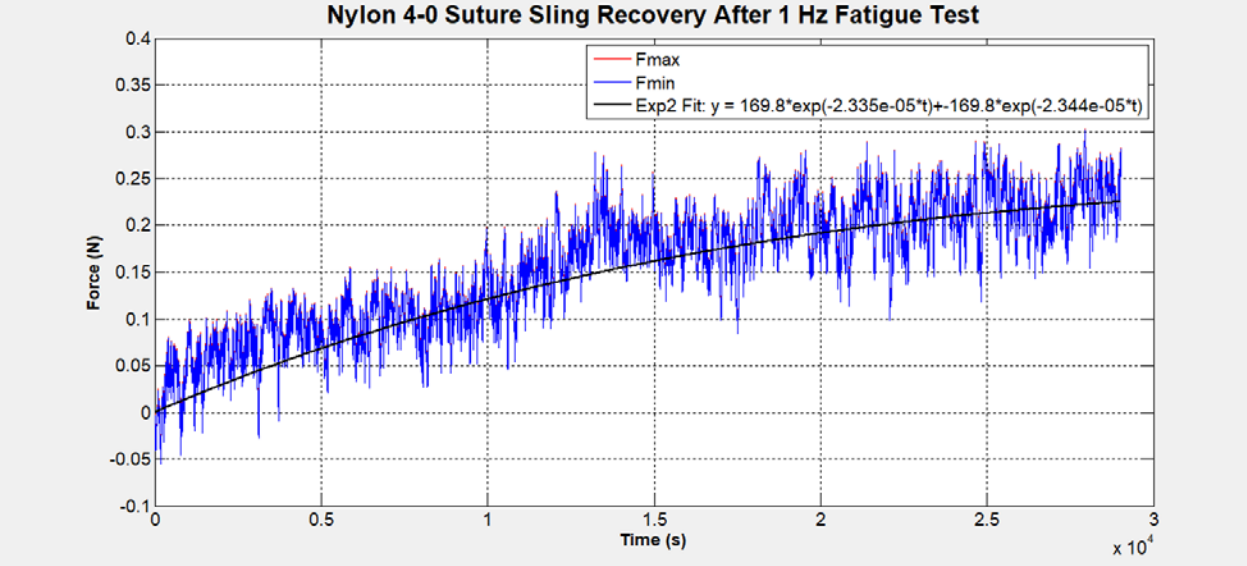

Figure 34: Recovery of the load for a nylon monofilament 4-0 suture sling specimen after stopping the fatigue test.

Silicone rod frontalis suspension sling relaxation, fatigue, and recovery test results

After the bvi Visitec silicone rod frontalis suspension sling specimen was mounted securely to the grips, the heated bath was filled with saline solution. Testing began once the temperature of the solution reached 37°C and the load cell read-out stabilized. Afterwards, the upper grip was pulled to induce a 0.96 N force in the sling specimen. The specimen was then left in tension for an extended period of time and load changes inside the specimen were recorded. Figure 35 shows the result of a stress relaxation test for a silicone rod sling specimen. The tension imposed on the sling dropped to 0.90 N (~6% reduction in load) in about 30 minutes. The relaxation test can represent two cases regarding the sing behavior: one is the behavior of the sling just after its implantation in the body and before when the patient starts to blink, and a second is the behavior of the implanted sling when it undergoes extended periods of constant tension for example due to eye closure when

the patient is asleep. Stress relaxation during such periods does not change the load inside the sling significantly (just 6% drop in silicone compared to 30% drop in the case of nylon).

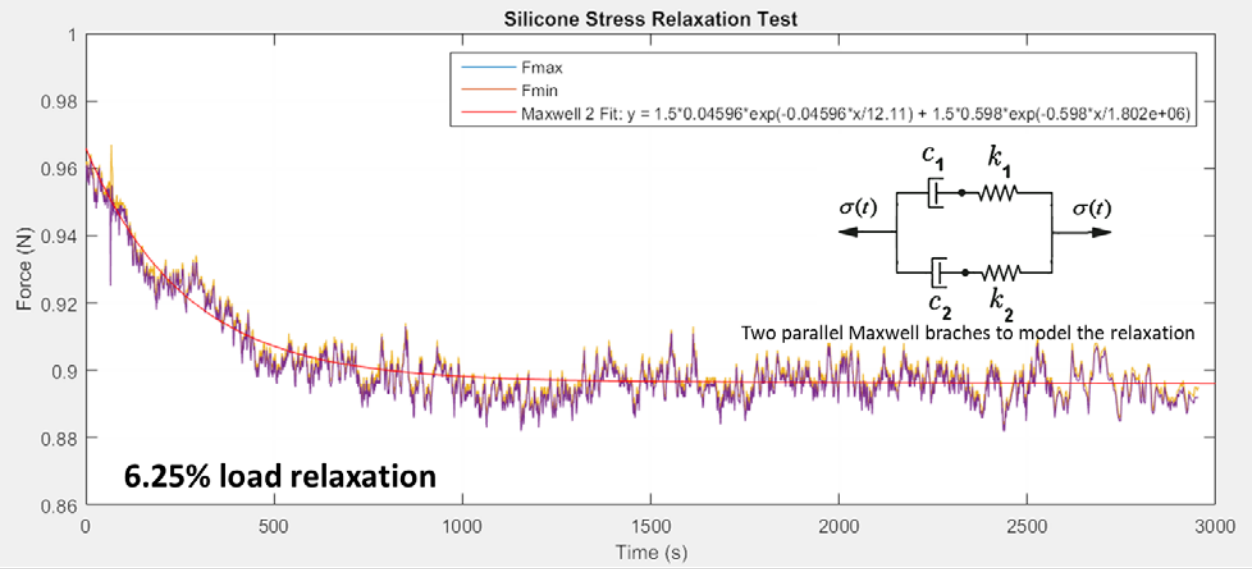

Sling type	Geometry and Cross section area (A) $[mm^2]$	Spring constant $[N/m]$	Maximum applied force $[N]$	Elasticity $[MPa]$	Maximum applied stress $[MPa]$
Silicone	D=0.9 mm A= 0.636	157.5	1.35	1.06	2.12

Silicone Stress Relaxation Test	
Coefficient	Value
ε_0	1.5
K_1	0.04596
C_1	12.11
K_2	0.598
C_2	1.802e+06

Figure 35: Stress relaxation in a silicone rod sling specimen

Although we performed fatigue tests with silicone slings under different loading frequencies and R-ratios (R-ratio = min strain or stress during the loading cycle divided by max strain or stress during the loading cycle), here we just report the result of fatigue test in 1 Hz mode and R-ratio = 0.71 N / 1.36 N = 0.52 (see Figure 36). Interestingly, F_{max} dropped from ~1.36 N to ~1.26 N just in the first 10 cycles. After this sharp drop in stress in the first few cycles, F_{max} gradually dropped to ~1.15 N exponentially and stabilized during ~ 4×10^3 cycles.

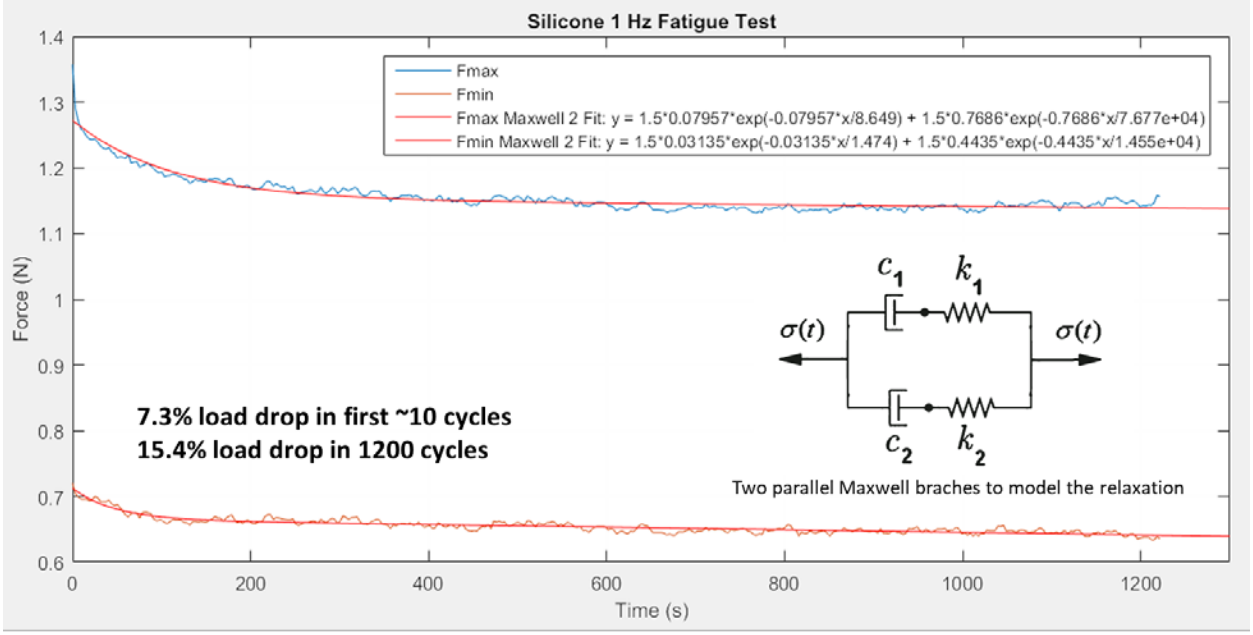

Silicone F_{max} 1 Hz Fatigue Test	
Coefficient	Value
ε_0	1.5
K_1	0.07957
C_1	8.649
K_2	0.7686
C_2	7.677e+04

Silicone F_{min} 1 Hz Fatigue Test	
Coefficient	Value
ε_0	1.5
K_1	0.03135
C_1	1.474
K_2	0.4435
C_2	1.455e+04

Figure 36: Fatigue test result for a silicone rod sling specimen at 1 Hz

Immediately following the fatigue test, we allowed the silicone sling specimen to sit at its position of minimum strain (F_{min} position) to determine whether or not there was any recovery in the load. It was noticed that there was almost no recovery as shown in Figure 37.

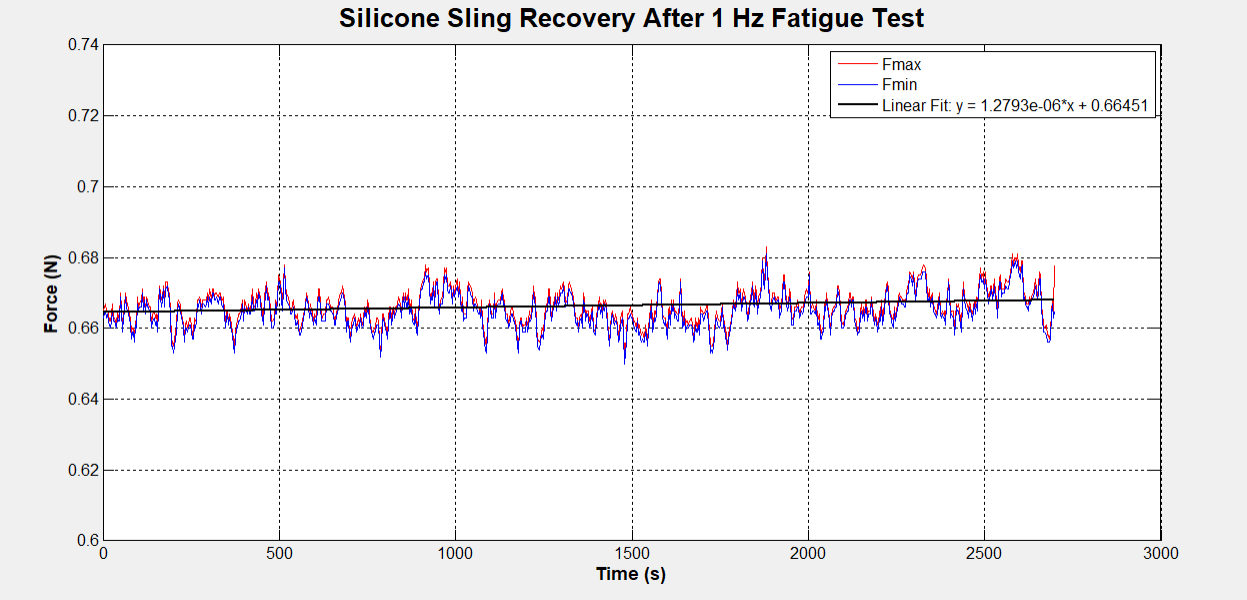

Figure 37: Recovery of the load for a silicone sling specimen after stopping the fatigue test.

Fascia lata relaxation, fatigue, and recovery test results

Results of relaxation, fatigue, and recovery tests are presented in the following for a banked fascia lata specimen. After a banked fascia lata sling specimen was mounted securely to the grips, the saline bath was filled by saline solution. Testing began once the temperature of the solution reached 37°C and the load cell read-out stabilized. Afterwards, the upper grip was pulled to induce a 0.22 N force in the sling specimen. Several trial and error cases led us to choose this initial induced force in the fascia lata sling specimen that is much smaller compared to the force initially induced in nylon and silicone samples before. Larger forces could lead to structural damage and significant rupture of some the fibers in the fascia lata specimen during the first transition from F_{min} position to F_{max} position.

The specimen was then left in tension for an extended period of time and load changes inside the specimen were recorded. Figure 35 shows the result of stress relaxation test of silicone rod sling specimen. The tension inside the sling dropped to 0.90 N (~6% reduction in the load) in approximately 30 minutes. The relaxation test can represent two cases regarding the sling behavior: one is the behavior of the sling just after its implantation in the body and before when the patient starts to blink, and second is the behavior of the implanted sling when it undergoes extended periods of constant tension for example due to eye closure when the patient is asleep. Stress relaxation during such periods does not change the load inside the sling significantly (just 6% drop in silicone compared to 30% drop in nylon case).

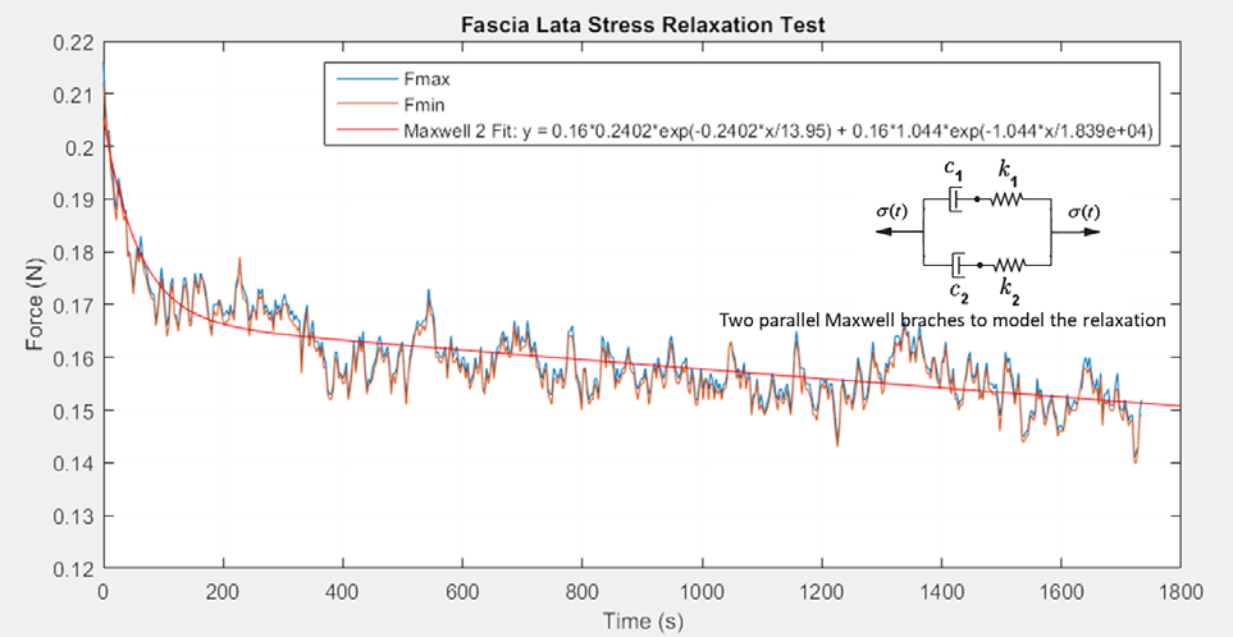

Sling type	Geometry and Cross section area (A) $[mm^2]$	Spring constant $[N/m]$	Maximum applied force $[N]$	Elasticity $[MPa]$	Maximum applied stress $[MPa]$
Fascia Lata	W = 3 mm t = 0.41 mm A= 1.23	1015	4.21	20.6	3.42

Fascia Lata Stress Relaxation Test	
Coefficient	Value
ϵ_0	0.16
K_1	0.2402
C_1	13.95
K_2	1.044
C_2	1.839e+04

Figure 38: Stress relaxation for a fascia lata sling specimen

Although we performed fatigue test of silicone sling at different loading frequencies and R-ratios (R-ratio = min strain or stress during the loading cycle divided by max strain or stress during the loading cycle), here we just report the result of a fatigue test in 1 Hz mode and R-ratio = 0.71 N / 1.36 N = 0.52 (see Figure 36). Interestingly, F_{max} dropped from ~1.36 N to ~1.26 N just in the first 10 cycles. After this sharp drop in stress in the first few cycles, F_{max} gradually dropped to ~1.15 N exponentially and stabilized during ~ 4×10^3 cycles.

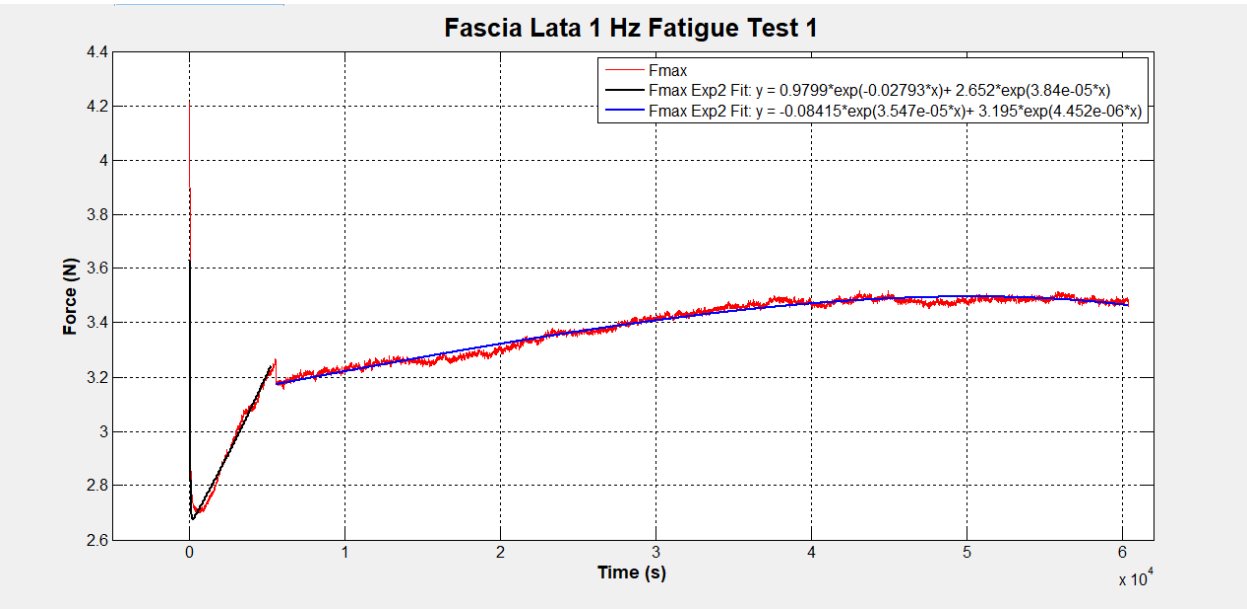

Figure 39: Fatigue test result for a fascia lata specimen at 1 Hz

The results mentioned in this chapter show that study of the load changes in the sling materials can provide useful information for predicting the behavior of the slings when they are stretched for an extended amount of the time or when they are under eye blinking induced cyclic loading.

Chapter 6

Conclusion

In this work, we hypothesized that mechanical and material property changes to the sling materials used to suspend the eyelid in patients suffering blepharoptosis can be a reason for recurrence of blepharoptosis after performing frontalis suspension surgery in them.

Specifically, we were interested to understand whether eye blinking can be a factor contributing to the recurrence. Considering that an average person blinks every 5 seconds, the implanted eyelid sling undergoes millions of loading and unloading cycles each year. Although the load needed to open and close the eye is in the range of at most a few Newtons, the cyclic behavior of this loading causes physical changes in the sling material. In order to investigate this hypothesis we developed two different experimental setups. Different sling materials were tested and characterized using these setups. Basically, the incident of plastic elongation, relaxation, and anelastic elongation in the sling materials were of interest.

The first experimental setup was a proof-of-concept preliminary setup aimed to measure the occurred plastic elongation in the sling samples under fatigue conditions caused by eye blinking

in the sling samples. We were able to prove via the experiments done by the preliminary setup that plastic elongation may occur in the sling specimens under cyclic loading in the range of the load needed to open and close the eyes. We could show that different sling materials exhibit different plastic elongation rates. The results from the preliminary setup showed that crazing and other structural changes might occur in the slings made of polymers of nylon family. These changes could cause significant issues to the tissue surrounding the sling like cheese-wiring or cutting through the tissue. Moreover, we could confirm that fresh and processed fascia lata could exhibit significantly different behaviors under fatigue conditions; of course, the processing protocol on the fascia lata specimen influences its behavior.

The second in-vitro setup made it possible to perform fatigue testing of different sling materials in more physiologically relevant conditions. In this second experimental setup, the load changes in the sling material under cycling loading mimicking the loads in the implanted slings in the eye were studied in a more controlled way. Here, we tested different sling materials under different strain amplitudes and strain rates. We were able to show that stress relaxation happens in all the studied sling samples. The load imposed on the silicone under both stress relaxation and cyclic loading reaches steady state condition faster than nylon and fascia lata. Moreover, the percentage of the load drop for silicone is less than that for nylon and fascia lata. We were able to show that some extent of load recovery in the sling specimen occurs after stopping the fatigue tests. The load recovery percentage is larger in nylon comparing to silicone. Silicone almost shows no load recovery after stopping the cyclic loading condition.

We were able to show that in all the materials, the first few cyclic loadings have a significant effect. This proves how much preconditioning the slings before implanting them inside the body is important. Applying different preconditioning protocols to the slings before implantation can

lead to significant effects on over-correction or under-correction after surgery. We suggest that a preconditioning protocol should be standardized to reduce the amount of sling failures after the frontalis suspension procedure. Last but not least, we noticed that fascia lata represents different behavior under fatigue condition compared to silicone and nylon. It can become stiffer and stronger due to cyclic loading. There needs to be more investigation on why fascia lata exhibits this unexpected behavior. Specifically, performing more experiments with different specimens of fascia lata (fresh and processed using different protocols) can shed more light on this interesting phenomenon.

Chapter 7

Future Work

Future work is suggested in the following:

1- Other sling materials depending on the availability should also be tested.

2- New materials for the frontalis suspension sling should be investigated. Based on the result of the present work, the ideal material will provide better resistance to plastic elongation. It would be beneficial if the candidate material has a shape memory property. This may give the surgeon the capability to adjust the sling even after implanting it in the patient body. One of our suggestions for this material is NiTi shape memory alloys. The superelastic behavior of NiTi makes it a suitable material resistant to plastic elongation caused by cyclic loadings caused due to eye blinking. Moreover, the shape memory effect of NiTi might be suitable to actively change the implanted sling length [92]–[98].

3- As NiTi is a metal and can cause cheese-wiring effects to the tissue surrounding the sling, we have proposed coating the NiTi sling with silicone. This way, the sling will be

composed of a core made of NiTi alloy covered by a sheath of silicone polymer. Silicone polymer will hinder the cheese-wiring caused by stiff NiTi part of the sling.

4- Different sling loop design such as Crawford triangles, rhomboid, Fox Pentagon could also be investigated under simulated physiological conditions. The grip design and geometry could be adjusted in our setup to accommodate different loop designs.

5- Wear studies of the implanted sling materials could also be investigated by our setup. The sling specimen could be passed over the some type of material with the same wearing property of the tissue surrounding the sling. Also, the sling specimen could be passed through a hollow cylinder that its internal surface has wearing characteristics the same as the tissue surrounding the sling. As an example for the material that has the same wearing properties as the tissue surrounding the sling, PDMS polymer could be used. The elasticity and wearing coefficient of PDMS is adjustable by changing the ratio of elastomer and resin.

6- All the tests conducted in the present work were based on strain-controlled fatigue tests. Stress-controlled fatigue tests could also be performed to simulate those cases that the force applied by the frontalis muscle to the sling is constant during the implantation of the sling.

7- In the present work, a sinusoidal or close to sinusoidal loading profile was applied to the slings for cyclic loading. With this current setup, the load profile could not be adjusted unless for loading frequencies less than 3 Hz. However, loading profile could be defined and adjusted in the electroforce fatigue test instruments (from TA instruments [99]). Provided having access to an electroforce fatigue test instrument, palpebral aperture profile (as the one provided in [100]) with respect to time could be used as the loading profile in strain-controlled fatigue tests.

8- More experiments need to be done to find the effect of frequency on the fatigue life of sling samples. These studies could also help with finding the optimum frequency for testing the sling materials.

9- Numerous clinical studies have investigated different sling materials used in frontalis suspension retrospectively. However, no prospective studies have yet be done on sling materials. We propose a prospective study on the mechanical and material changes in the slings and correlating that with the recurrence of ptosis. The slings length could be measured before implantation in the patient. Also, SEM images of the sling could be taken before the surgery. After the surgery, the patients will be followed up. In those patients who experience recurrence of ptosis and need to undergo the surgery again, the older sling can be measured and imaged after the extraction. Comparing the results of these measurements and images before implantation and after extraction may reveal some insight to whether plastic elongation or other physical and material changes happen to them.

10- Based on the insights from the present work and future studies, appropriate protocols for preconditioning of the sling specimens before implanting inside the body should be developed.

11- More investigation could be performed to come up with a reasonable modeling and explanation for the occurrence of recovery after the fatigue tests in nylon samples.

12- The fatigue test system that we developed for study of sling materials used in frontalis suspension could be used for studies related to other biomedical implants that undergo cyclic loading while implanted in the body. Some examples could be the sutures and slings that are used in other parts of the body or various catheters.

13- The proof-of-concept fatigue setup that was developed based on a sewing machine could be a cheap option for other fatigue tests even not related to biomedical applications.

Bibliography

[1] Y. Takahashi, I. Leibovitch, and H. Kakizaki, “Frontalis suspension surgery in upper eyelid blepharoptosis.,” *Open Ophthalmol. J.*, vol. 4, pp. 91–97, 2010.

[2] P. Sudhakar, Q. Vu, O. Kosoko-Lasaki, and M. Palmer, “Upper Eyelid Ptosis Revisited,” *Am. J. Clin. Med.*, vol. 6, no. 3, pp. 5–14, 2009.

[3] G. C. Gusek-Schneider and P. Martus, “Stimulus deprivation amblyopia in human congenital ptosis: a study of 100 patients.,” *Strabismus*, vol. 8, no. 4, pp. 261–70, Dec. 2000.

[4] R. L. Anderson and S. A. Baumgartner, “Amblyopia in ptosis.,” *Arch. Ophthalmol. (Chicago, Ill. 1960)*, vol. 98, no. 6, pp. 1068–9, Jun. 1980.

[5] G. J. Ben Simon, A. a Macedo, R. M. Schwarcz, D. Y. Wang, J. D. McCann, and R. a Goldberg, “Frontalis suspension for upper eyelid ptosis: evaluation of different surgical designs and suture material.,” *Am. J. Ophthalmol.*, vol. 140, no. 5, pp. 877–85, Nov. 2005.

[6] S. F. Ho, A. Morawski, R. Sampath, and J. Burns, “Modified visual field test for ptosis surgery (Leicester Peripheral Field Test).,” *Eye (Lond).*, vol. 25, no. 3, pp. 365–9, Mar. 2011.

[7] “Blepharoptosis - EyeWiki.” [Online]. Available: http://eyewiki.aao.org/Blepharoptosis.

[8] C. Morris, “Acquired Ptosis: Evaluation and Management - American Academy of Ophthalmology,” *AAO*, 2005. [Online]. Available: https://www.aao.org/eyenet/article/acquired-ptosis-evaluation-management.

[9] T. Fujiwara, K. Matsuo, S. Kondoh, and S. Yuzuriha, “Etiology and pathogenesis of

aponeurotic blepharoptosis.,” *Ann. Plast. Surg.*, vol. 46, no. 1, pp. 29–35, Jan. 2001.

[10] P. L. Custer, R. R. Tenzel, and A. P. Kowalczyk, “Blepharochalasis syndrome.,” *Am. J. Ophthalmol.*, vol. 99, no. 4, pp. 424–8, Apr. 1985.

[11] R. L. Arden and G. K. Moore, “Complete post-traumatic ptosis: A mechanism for recovery?,” *Laryngoscope*, vol. 99, no. 11, pp. 1175–1179, Nov. 1989.

[12] J. Dutton, *A Color Atlas of Ptosis: A Practical Guide to Evaluation and Management*. Lucky Plaza, Singapore: P.G. Publishing Pte Ltd., 1989.

[13] J. Finsterer, “Ptosis: Causes, Presentation, and Management,” *Aesthetic Plast. Surg.*, vol. 27, no. 3, pp. 193–204, Jun. 2003.

[14] J. Roberts and E. M. Ahuja, *Hearing sensitivity and related medical findings among youths 12-17 years, United States*. U.S. Dept. of Health, Education, and Welfare, Public Health Service, Health Resources Administration, National Center for Health Statistics, 1975.

[15] B. M. Hosal, O. Tekeli, and E. Gürsel, “Eyelid malpositions after cataract surgery.,” *Eur. J. Ophthalmol.*, vol. 8, no. 1, pp. 12–5.

[16] J. D. Bullock, R. E. Warwar, D. G. Bienenfeld, S. L. Marciniszyn, and R. J. Markert, “PSYCHOSOCIAL IMPLICATIONS OF BLEPHAROPTOSIS AND DERMATOCHALASIS*,” *Ophth. Soc. Tr Am Ophth Soc*, vol. 9999, pp. 65–72, 2001.

[17] B. C. Edmonson, A. E. Wulc, A. Harrison, and et al., “Ptosis evaluation and management.,” *Otolaryngol. Clin. North Am.*, vol. 38, no. 5, pp. 921–46, Oct. 2005.

[18] K. Tarbet, B. Lemke, D. Albert, F. Jakobiec, D. Azar, and E. Gragoudas, “Anatomy of the eyelids and lacrimal drainage system,” in *Principles and practice of ophthalmology*, 2000, pp. 3318–3332.

[19] J. B. Holds, A. G. Buchanan, M. Hartstein, D. A. Weinberg, and A. J. Cohen, “Evaluation and Management of Blepharoptosis,” pp. 253–262, 2011.

[20] “World Optic - Ptosis Eye Crutches.” [Online]. Available:

https://www.worldoptic.com/adjust-glasses-modify-eyewear/eyeglasses-ptosis-drooping-eye-lid-crutches.php#.WY6iuYjyvIW.

[21] “The fastest moving muscle in the human body - Whats What.” [Online]. Available: http://vivawhatswhat.com/fastest-moving-muscle-human-body/.

[22] “A Primer on Ptosis.” [Online]. Available: http://webeye.ophth.uiowa.edu/eyeforum/tutorials/Ptosis/index.htm.

[23] “Eyelid Anatomy and Function | Clinical Gate.” [Online]. Available: https://clinicalgate.com/eyelid-anatomy-and-function/.

[24] J. Crawford, “Repair of ptosis using frontalis muscle and fascia lata: a 20-year review.,” *Ophthalmic Surg.*, vol. 8, no. 4, pp. 31–40, 1977.

[25] U. P. Press and H. Hübner, “Maximal levator resection in the treatment of unilateral congenital ptosis with poor levator function.,” *Orbit*, vol. 20, no. 2, pp. 125–129, Jun. 2001.

[26] M. Baroody, J. B. Holds, and V. L. Vick, “Advances in the diagnosis and treatment of ptosis.,” *Curr. Opin. Ophthalmol.*, vol. 16, no. 6, pp. 351–5, Dec. 2005.

[27] “Measurement levator function.” [Online]. Available: http://cursoenarm.net/UPTODATE/contents/mobipreview.htm?24/54/25443.

[28] D. H. Park, W. S. Choi, S. H. Yoon, and J. S. Shim, “Comparison of Levator Resection and Frontalis Muscle Transfer in the Treatment of Severe Blepharoptosis,” *Ann. Plast. Surg.*, vol. 59, no. 4, pp. 388–392, Oct. 2007.

[29] C. A. Cates and A. G. Tyers, “Outcomes of anterior levator resection in congenital blepharoptosis,” *Eye*, vol. 15, no. 6, pp. 770–773, Nov. 2001.

[30] K. Spahiu, L. Spahiu, and E. Dida, “Choice of surgical procedure for ptosis correction.,” *Med. Arh.*, vol. 62, no. 5–6, pp. 283–4, 2008.

[31] O. Ural, M. Mocan, A. Dolgun, and U. Erdener, “The utility of margin-reflex distance in determining the type of surgical intervention for congenital blepharoptosis,” *Indian J.*

Ophthalmol., vol. 64, no. 10, p. 752, Oct. 2016.

[32] A. Cetinkaya and P. A. Brannan, “Ptosis repair options and algorithm,” *Curr. Opin. Ophthalmol.*, vol. 19, no. 5, pp. 428–434, Sep. 2008.

[33] S. R. Carter, W. J. Meecham, S. R. Seiff, and E. Arocker-Mettinger, “Silicone frontalis slings for the correction of blepharoptosis: indications and efficacy.,” *Ophthalmology*, vol. 103, no. 4, pp. 623–30, Apr. 1996.

[34] S. M. Betharia, “Frontalis sling: a modified simple technique.,” *Br. J. Ophthalmol.*, vol. 69, no. 6, pp. 443–5, Jun. 1985.

[35] A. Ahmadi and B. Sires, “Ptosis in infants and children,” *Int Ophthalmol Clin*, vol. 42, pp. 15–29, 2002.

[36] J. a Sokol, I. L. Thornton, H. B. H. Lee, and W. R. Nunery, “Modified frontalis suspension technique with review of large series.,” *Ophthal. Plast. Reconstr. Surg.*, vol. 27, no. 3, pp. 211–215, 2011.

[37] J. S. FRIEDENWALD and J. S. GUYTON, “A simple ptosis operation; utilization of the frontalis by means of a single rhomboid-shaped suture.,” *Am. J. Ophthalmol.*, vol. 31, no. 4, pp. 411–4, Apr. 1948.

[38] W. Wright, “The use of living sutures in the treatment of ptosis,” *Arch Ophthalmol.*, vol. 51, pp. 99–102, 1922.

[39] S. Fox, *Surgery of Ptosis*. The Williams & Wilkins Company, 1980.

[40] K.-A. Kwon, R. J. Shipley, M. Edirisinghe, S. M. Best, R. E. Cameron, C. Poitelea, G. E. Rose, and D. G. Ezra, “The Mechanics of Brow-Suspension Ptosis Repair,” *Ophthal. Plast. Reconstr. Surg.*, vol. 33, no. 1, pp. 22–26, 2017.

[41] B. N. Wasserman, D. T. Sprunger, and E. M. Helveston, “Comparison of materials used in frontalis suspension.,” *Arch. Ophthalmol.*, vol. 119, no. 5, pp. 687–91, May 2001.

[42] C. Y. Kim, B. J. Son, J. Son, J. Hong, and S. Y. Lee, “Analysis of the causes of recurrence after frontalis suspension using silicone rods for congenital ptosis,” *PLoS One*, vol. 12, no.

2, p. e0171769, Feb. 2017.

[43] B. Esmaeli, H. Chung, and R. C. Pashby, “Long-Term Results of Frontalis Suspension Using Irradiated, Banked Fascia Lata,” *Ophthalmic Plast. Reconstr. Surg.*, vol. 14, no. 3, pp. 159–163, May 1998.

[44] E. Pacella, D. Mipatrini, F. Pacella, G. Amorelli, A. Bottone, G. Smaldone, P. Turchetti, and G. La Torre, “Suspensory Materials for Surgery of Blepharoptosis: A Systematic Review of Observational Studies,” *PLoS One*, vol. 11, no. 9, p. e0160827, Sep. 2016.

[45] R. Wagner, J. J. Mauriello, L. Nelson, and E. Al., “Treatment of congenital ptosis with frontalis suspension: a comparison of suspensory materials,” *Ophthalmology*, vol. 91, pp. 245–248, 1984.

[46] M. Wilson and R. Johnson, “Congenital ptosis: long-term results of treatment using lyophilized fascia lata for frontalis suspension,” *Ophthalmology*, vol. 98, p. 1234 –1237., 1991.

[47] P. Metha, P. Patel, and J. Olver, “Functional results and complications of Polyester mesh use for frontalis suspension ptosis surgery,” *Br J Ophthalmol*, vol. 88, pp. 361–364, 2004.

[48] D. Liu, “Blepharoptosis correction with frontalis suspension using a nylon monofilament sling: duration of effect,” *Am J Ophthalmol*, vol. 128, pp. 772–773, 1999.

[49] M. J. Doughty and T. Naase, “Further Analysis of the Human Spontaneous Eye Blink Rate by a Cluster Analysis-Based Approach to Categorize Individuals With ???Normal??? Versus ???Frequent??? Eye Blink Activity,” *Eye Contact Lens Sci. Clin. Pract.*, vol. 32, no. 6, pp. 294–299, 2006.

[50] I. Fatt and B. A. Weissman, *Physiology of the Eye: An Introduction to the Vegetative Functions, Second ed.* 1992.

[51] J. M. Anderson, A. Rodriguez, and D. T. Chang, “Foreign body reaction to biomaterials.,” *Semin. Immunol.*, vol. 20, no. 2, pp. 86–100, Apr. 2008.

[52] “USP Monographs: Nonabsorbable Surgical Suture.” [Online]. Available:

http://www.pharmacopeia.cn/v29240/usp29nf24s0_m80200.html.

[53] “Suture Sizes.” [Online]. Available: http://www.dolphinsutures.com:8080/suture-sizes. [Accessed: 07-Aug-2017].

[54] D. E. Holmlund, “Physical properties of surgical suture materials: Stress-strain relationship, stress-relaxation and irreversible elongation.,” *Ann. Surg.*, vol. 184, no. 2, pp. 189–93, Aug. 1976.

[55] J. S. Temenoff and A. G. Mikos, *Biomaterials: The Intersection of Biology and Materials Science*. Upper Saddle River, NJ: Pearson, 2008.

[56] T. Nilsson, “Mechanical properties of Prolene, Ethilion and surgical steel loops.,” *Scand. J. Plast. Reconstr. Surg.*, vol. 15, no. 2, pp. 111–5, 1981.

[57] T. Nilsson, “Mechanical Properties of Prolene® and Ethilon® Sutures After Three Weeks in Vivo,” *Scand. J. Plast. Reconstr. Surg.*, vol. 16, no. 1, pp. 11–15, Jan. 1982.

[58] D. Greenwald, S. Shumway, P. Albear, and L. Gottlieb, “Mechanical Comparison of 10 Suture Materials before and after in Vivo Incubation,” *J. Surg. Res.*, vol. 56, no. 4, pp. 372–377, Apr. 1994.

[59] F. Vizesi, C. Jones, N. Lotz, M. Gianoutsos, and W. R. Walsh, “Stress Relaxation and Creep: Viscoelastic Properties of Common Suture Materials Used for Flexor Tendon Repair,” *J. Hand Surg. Am.*, vol. 33, no. 2, pp. 241–246, Feb. 2008.

[60] K.-A. Kwon, R. J. Shipley, M. Edirisinghe, D. G. Ezra, G. E. Rose, A. W. Rayment, S. M. Best, and R. E. Cameron, “Microstructure and mechanical properties of synthetic brow-suspension materials,” *Mater. Sci. Eng. C*, vol. 35, pp. 220–230, Feb. 2014.

[61] K.-A. Kwon, R. J. Shipley, M. Edirisinghe, A. W. Rayment, S. M. Best, R. E. Cameron, T. Salam, G. E. Rose, and D. G. Ezra, “Stress-relaxation and fatigue behaviour of synthetic brow-suspension materials,” *J. Mech. Behav. Biomed. Mater.*, vol. 42, pp. 116–128, 2015.

[62] H. Chaudhry, C.-Y. Huang, R. Schleip, Z. Ji, B. Bukiet, and T. Findley, “Viscoelastic

behavior of human fasciae under extension in manual therapy," *J. Bodyw. Mov. Ther.*, vol. 11, no. 2, pp. 159–167, Apr. 2007.

[63] K. Maksymowicz, K. Marycz, S. Szotek, K. Kaliński, E. Serwa, R. Łukomski, and J. Czogała, "Chemical composition of human and canine fascia lata.," *Acta Biochim. Pol.*, vol. 59, no. 4, pp. 531–5, 2012.

[64] D. L. Butler, E. S. Grood, F. R. Noyes, R. F. Zernicke, and K. Brackett, "Effects of structure and strain measurement technique on the material properties of young human tendons and fascia.," *J. Biomech.*, vol. 17, no. 8, pp. 579–96, 1984.

[65] R. W. Bright and W. T. Green, "Freeze-dried fascia lata allografts: a review of 47 cases.," *J. Pediatr. Orthop.*, vol. 1, no. 1, pp. 13–22, 1981.

[66] E. H. Bedrossian, "Banked fascia lata as an orbital floor implant.," *Ophthal. Plast. Reconstr. Surg.*, vol. 9, no. 1, pp. 66–70, 1993.

[67] V. L. Handa, J. K. Jensen, M. M. Germain, and D. R. Ostergard, "Banked human fascia lata for the suburethral sling procedure: a preliminary report.," *Obstet. Gynecol.*, vol. 88, no. 6, pp. 1045–9, Dec. 1996.

[68] W. T. Green, "Fascia grafts.," *Transplant. Proc.*, vol. 8, no. 2 Suppl 1, pp. 113–8, Jun. 1976.

[69] D. W. Jackson, E. S. Grood, P. Wilcox, D. L. Butler, T. M. Simon, and J. P. Holden, "The effects of processing techniques on the mechanical properties of bone-anterior cruciate ligament-bone allografts," *Am. J. Sports Med.*, vol. 16, no. 2, pp. 101–105, Mar. 1988.

[70] J. M. Choe and T. Bell, "Genetic material is present in cadaveric dermis and cadaveric fascia lata.," *J. Urol.*, vol. 166, no. 1, pp. 122–4, Jul. 2001.

[71] C. M. Gratz, "Tensile Strength and elasticity tests on human fascia lata," *J. Bone Jt. Surg.*, vol. 13, no. 2, pp. 334–340, 1931.

[72] W. E. Gallie and A. B. Lemesurier, "The Use of Living Sutures in Operative Surgery.," *Can. Med. Assoc. J.*, vol. 11, no. 7, pp. 504–13, Jul. 1921.

[73] E. D. Thomas and R. B. Gresham, “Comparative Tensile Strength Study of Fresh, Frozen, and Freeze-Dried Human Fascia Lata.,” *Surg. Forum*, vol. 14, pp. 442–3, 1963.

[74] R. Hinton, R. H. Jinnah, C. Johnson, K. Warden, and H. J. Clarke, “A biomechanical analysis of solvent-dehydrated and freeze-dried human fascia lata allografts,” *Am. J. Sports Med.*, vol. 20, no. 5, pp. 607–612, Sep. 1992.

[75] K. A. Derwin, A. R. Baker, R. K. Spragg, D. R. Leigh, W. Farhat, and J. P. Iannotti, “Regional variability, processing methods, and biophysical properties of human fascia lata extracellular matrix,” *J. Biomed. Mater. Res. Part A*, vol. 84A, no. 2, pp. 500–507, Feb. 2008.

[76] A. Aurora, M. Mesiha, C. D. Tan, E. Walker, S. Sahoo, J. P. Iannotti, J. A. McCarron, and K. A. Derwin, “Mechanical characterization and biocompatibility of a novel reinforced fascia patch for rotator cuff repair,” *J. Biomed. Mater. Res. Part A*, vol. 99A, no. 2, pp. 221–230, Nov. 2011.

[77] S. Suresh, *Fatigue of Materials*, 2nd ed. Cambridge, UK: Cambridge University Press, 1998.

[78] C. Evereklioglu, “‘Kite-tail’ fascia lata strips technique: frontalis suspension using a non-endoscopic minimally invasive single-thigh incision approach.,” *Br. J. Ophthalmol.*, vol. 96, no. 4, pp. 570–575, 2012.

[79] K.-A. Kwon, R. J. Shipley, M. Edirisinghe, D. G. Ezra, G. Rose, S. M. Best, and R. E. Cameron, “High-speed camera characterization of voluntary eye blinking kinematics.,” *J. R. Soc. Interface*, vol. 10, no. 85, p. 20130227, 2013.

[80] M. J. Lee, J. Y. Oh, H.-K. Choung, N. J. Kim, M. S. Sung, and S. I. Khwarg, “Frontalis Sling Operation Using Silicone Rod Compared with Preserved Fascia Lata for Congenital Ptosis,” *Ophthalmology*, vol. 116, no. 1, pp. 123–129, Jan. 2009.

[81] M. D. Abràmoff, P. J. Magalhães, and S. J. Ram, “Image processing with imageJ,” *Biophotonics Int.*, vol. 11, no. 7, pp. 36–41, 2004.

[82] H. H. Kausch and C. Oudet, “Progress and challenge in polymer crazing and fatigue,”

Makromol. Chemie. Macromol. Symp., vol. 22, no. 1, pp. 207–224, Oct. 1988.

[83] T. C. B. McLeish, C. J. G. Plummer, and A. M. Donald, “Crazing by disentanglement: non-diffusive reptation,” *Polymer (Guildf).*, vol. 30, no. 9, pp. 1651–1655, Sep. 1989.

[84] P. A. O’Connell and G. B. Mckenna, *Encyclopedia of Polymer Science and Technology*, 4th editio. New York, NY: John Wiley & Sons, Inc., 2014.

[85] K. H. Kook, H. Lew, J. H. Chang, H. Y. Kim, J. Ye, and S. Y. Lee, “Scanning electron microscopic studies of Supramid Extra from the patients displaying recurrent ptosis after frontalis suspension,” *Am. J. Ophthalmol.*, vol. 138, pp. 756–763, 2004.

[86] ASTM Compass, “ASTM D5034 - 09 (2013): Standard Test Method for Breaking Strength and Elongation of Textile Fabrics (Grab Test).” [Online]. Available: www.astm.org.

[87] A. Compass, “ASTM E606/E606M-12 Standard Test Method for Strain-Controlled Fatigue Testing, ASTM International, West Conshohocken, PA, 2012, https://doi.org/10.1520/E0606_E0606M-12.” [Online]. Available: ASTM E606/E606M-12 Standard Test Method for Strain-Controlled Fatigue Testing, ASTM International, West Conshohocken, PA, 2012, https://doi.org/10.1520/E0606_E0606M-12.

[88] P. A. Schmidt, E. C. V. S. Division, B. Healthcare, R. H. Avenue, and J. C. Earthman, “Development of a scanning laser crack detection technique for corrosion fatigue testing of fine wire,” *Development*, 1995.

[89] V. B. Markov, B. D. Buckner, and J. C. Earthman, “<title>Laser scanning technique for fatigue damage evolution detection</title>,” vol. 5776, pp. 746–756, 2005.

[90] C. W. Senders, T. T. Tollefson, S. Curtiss, A. Wong-Foy, H. Prahlad, and N. F, “Force Requirements for Artificial Muscle to Create an Eyelid Blink With Eyelid Sling,” *Arch. Facial Plast. Surg.*, vol. 12, no. 1, pp. 91–94, Jan. 2010.

[91] H. B. Jacobs, “Strength of the orbicularis oculi.,” *Br. J. Ophthalmol.*, vol. 38, no. 9, pp. 560–6, Sep. 1954.

[92] M. Es-Souni, M. Es-Souni, and H. Fischer-Brandies, “Assessing the biocompatibility of NiTi shape memory alloys used for medical applications,” *Anal. Bioanal. Chem.*, vol. 381, no. 3, pp. 557–567, Feb. 2005.

[93] H. Fischer, B. Vogel, and A. Welle, “Applications of shape memory alloys in medical instruments,” *Minim. Invasive Ther. Allied Technol.*, vol. 13, no. 4, pp. 248–253, Jan. 2004.

[94] M. Denton and J. C. Earthman, “Corrosion evaluation of wear tested nitinol wire,” *Mater. Sci. Eng. C*, vol. 25, no. 3, pp. 276–281, May 2005.

[95] Q. Li, Y. Zeng, and X. Tang, “The applications and research progresses of nickel–titanium shape memory alloy in reconstructive surgery,” *Australas. Phys. Eng. Sci. Med.*, vol. 33, no. 2, pp. 129–136, Jun. 2010.

[96] M. Amarandei, L. Bogdan, A. Cernescu, L. Marşavina, J. M. Pătraşcu, and D. Vermeşan, “Experimental Tests on Fine Nitinol Wires Used in Medical Applications,” *Solid State Phenom.*, vol. 188, pp. 65–69, May 2012.

[97] L. B. Pértile, P. M. S. Silva, V. B. Peccin, R. Peres, P. G. Silveira, C. Giacomelli, F. C. Giacomelli, M. C. Fredel, and A. Spinelli, “In vivo human electrochemical properties of a NiTi-based alloy (Nitinol) used for minimally invasive implants,” *J. Biomed. Mater. Res. Part A*, vol. 89A, no. 4, pp. 1072–1078, Jun. 2009.

[98] Y. Ng, S. M. Shimi, N. Kernohan, T. G. Frank, P. A. Campbell, D. Martin, J. Gove, and A. Cuschieri, “Skin wound closure with a novel shape-memory alloy fixator,” *Surg. Endosc.*, vol. 20, no. 2, pp. 311–315, Feb. 2006.

[99] TA Instruments, “ElectroForce Mechanical Test Instruments – TA Instruments.” [Online]. Available: http://www.tainstruments.com/products/electroforce-mechanical-testers/.

[100] K.-A. Kwon, R. J. Shipley, M. Edirisinghe, D. G. Ezra, G. Rose, S. M. Best, and R. E. Cameron, “High-speed camera characterization of voluntary eye blinking kinematics,” *J. R. Soc. Interface*, vol. 10, no. 85, 2013.